Soil & Tillage Research 236 (2024) 105941

Contents lists available at ScienceDirect

Soil & Tillage Research

journal homepage: www.elsevier.com/locate/still

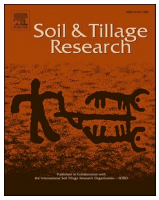

Wind erosion after steppe conversion in Kazakhstan

Moritz Koza [a,*], Roger Funk [b], Julia Pöhlitz [a], Christopher Conrad [a], Olga Shibistova [c], Tobias Meinel [d], Kanat Akshalov [e], Gerd Schmidt [a]

[a] Department of Geoecology, Institute of Geosciences and Geography, Martin Luther University Halle-Wittenberg, 06120 Halle (Saale), Germany
[b] Landscape Pedology, Leibniz Centre for Agricultural Landscape Research (ZALF), 15374 Müncheberg, Germany
[c] Institute of Soil Science, Leibniz University Hanover, 30419 Hanover, Germany
[d] Amazonen-Werke H. Dreyer SE & Co. KG, 49205 Hasbergen, Germany
[e] Soil and Crop Management, Barayev Research and Production Center for Grain Farming, 474010 Shortandy, Kazakhstan

ARTICLE INFO

Keywords:
Wind tunnel
On-farm experimentation
Soil management
Soil loss
Particle size distribution
Soil organic carbon

ABSTRACT

Semi-arid regions of Central Asia suffer from wind erosion due to expanding steppe conversion and unsustainable farming practices. Empirical data from field observations are needed to support the implementation of adapted management. In this study, a mobile wind tunnel was used for the first time in Kazakhstan to assess the soil's erodibility under real conditions. Field experiments were conducted on loamy sands with different initial conditions that are typical for the most erosive time of the year: a bare surface with a cloddy structure after recent steppe conversion, a weak crust on a plot with barley (*Hordeum vulgare L.*), and a plot with loose material in the rows of maize plants (*Zea mays L.*). Subsequently, different levels of mechanical stress (low, moderate, high) were considered to analyze the effect of disruptive forces soils experience during field cultivation (light cultivator, disc harrow, tractor tires) on possible soil losses. The results of wind tunnel experiments showed already great differences under initial conditions. The cloddy structure of the recent steppe conservation had the lowest susceptibility against wind erosion due to a good aggregation and a large roughness, resulting in soil loss of 12 g m^{-2}. The plot grown with barley was less affected by wind erosion due to the weak crust, smaller distances between plants, and leaves close to the ground (soil loss of 34 g m^{-2}). Maize was also the most problematic crop in the study area because wind can blow below the plant canopy without considerable resistance during the early growth stages. Additionally, existing deposits in the maize rows from previous erosion events led to the highest soil loss of 1609 g m^{-2}. Mechanical stress by seedbed preparation generally increased the erodible fraction, resulting in higher soil losses (light cultivator: 198 ± 129 g m^{-2}, disc harrow: 388 ± 258 g m^{-2}). The most severe disruption of soil structure occurred on tractor tire tracks, causing a loss of 2767 ± 1810 g m^{-2}. Consequently, the pulverizing effect of tractor tires on dry soil must be considered a serious emission source. Comparing the soil organic carbon content of topsoil and eroded material showed that organic carbon was enriched only in the aeolian sediments of the recently converted plot (+69%). We conclude that soils after steppe conversion need to be treated with particular care from the very beginning so that severe events from the past are not repeated.

1. Introduction

Soil degradation is an ongoing problem worldwide (Keesstra et al., 2016; Lal, 2001). Particular agriculture is often under the pressure of soil erosion, causing the redistribution of valuable topsoil, nutrients, and organic carbon (Cerdà et al., 2009; Montgomery, 2007). Aeolian processes usually occur without being noticed (Chepil, 1960; Funk et al., 2014) but data from global compilation surveys confirm that erosion rates from conventional agriculture are up to two times higher than soil production rates (Montgomery, 2007).

In the past, an extreme example has shown that soil cultivation can contribute to wind erosion, triggering a socio-ecological crisis (Peters et al., 2008). Known as the Dust Bowl Syndrome in the Great Plains of the USA during the 1930s, multiple natural and anthropogenic factors,

Abbreviations: ASD, aggregate size distribution; EF, erodible fraction; MWAC, Modified Wilson and Cook; PSD, particle size distribution; SOC, soil organic carbon; SUSTRA, Suspension Sediment Trap.

* Corresponding author.
E-mail address: moritz.koza@geo.uni-halle.de (M. Koza).

https://doi.org/10.1016/j.still.2023.105941
Received 27 April 2023; Received in revised form 24 October 2023; Accepted 31 October 2023
Available online 21 November 2023

including extensive steppe conversion, unsustainable farming practices and severe drought, caused devastating soil erosion on 20–40 million hectares (Hornbeck, 2012; McLeman et al., 2014; Zobeck et al., 2013). The Dust Bowl initially started on individual fields and turned into erosion among areas until it expanded to broad-scale events with land-atmosphere interactions (Peters et al., 2008), exceeding soil loss rates that have ever been recorded. Dust storms are still occurring in the Great Plains, but their current extent is far less concerning due to the adaptation of conservation tillage and no-till farming practices (Lal et al., 2007; Lee and Gill, 2015). Still, in many parts of the world, soil cultivation causes a considerable increase in wind erosion events (Shao, 2008).

The semi-arid steppe regions of Central Asia are challenged by soil erosion due to intense agriculture and extreme climate conditions (Reyer et al., 2017; Robinson, 2016). This is reinforced as climate models indicate an increase in the natural factors that promote wind erosion, such as higher temperatures and a change in precipitation patterns (Duulatov et al., 2021; Li et al., 2020b). Kazakhstan, in particular, faces an increasing risk of soil degradation due to wind erosion (Li et al., 2020b). Historically, northern Kazakhstan was part of the largest steppe conversion of the twentieth century (Virgin Lands Campaign, 1954–1963), where extensive grasslands were converted to arable land for grain production. Moldboard plowing was commonly used for steppe conversion and cultivation in order to increase spring wheat production, but it caused severe wind erosion and soil degradation (Meinel and Akshalov, 2015). Large areas of cropland were abandoned during the collapse of the Soviet Union (1991), but recent steppe conversion is expanding arable land again (Frühauf et al., 2020; Kraemer et al., 2015; Prishchepov et al., 2020). As a result, cascading effects may be possible as more land is exposed to wind erosion (Peters et al., 2008). Severe soil degradation in Kazakhstan could also threaten food security in Central Asia because of its important role as a grain exporter (FAO, 2012). Hence, soil erosion mitigation is an important step to ensure the achievement of the Sustainable Development Goals (Yin et al., 2022).

Assessments of erosion risks in the semi-arid steppe regions of Central Asia are rare (Borrelli et al., 2021), especially for wind erosion (Bezak et al., 2021; Field et al., 2009). However, they are necessary to develop adequate solutions. Field observations and laboratory tests from less-studied regions of the world can add to existing knowledge and provide useful benchmarks for building erosion models (Webb et al., 2020). Furthermore, empirical data are more accurate at smaller scales and can support sustainable management practices. For this purpose, we studied the wind erosion processes in the Kazakh Steppe in detail. In a recent study, we derived the potential erodibility of semi-arid steppe soils from aggregate stability tests. We could show that arable fields of northern Kazakhstan are susceptible to erosion, independent of their soil properties (Koza et al., 2022). In the present study, a mobile wind tunnel was used to assess the soil erodibility by wind under real conditions. Properly constructed and operated wind tunnels can be used to investigate the erodibility of the intact surface, with and without plant residues, as well as the disturbed soil under controlled and natural wind conditions (Zobeck and Van Pelt, 2015). In areas where continuous monitoring is difficult and reliable data are limited, data collected from mobile wind tunnel experiments offer a reasonable compromise to evaluate erosion risk, even if minor inaccuracies occur during the experimental setup (Marzen et al., 2020).

Wind erosion processes can be selective by removing the fine clay and silt-sized particles that contain disproportionately greater amounts of organic matter (Chappell et al., 2013; Zobeck and Fryrear, 1986). While the coarse sand fraction (>500 μm) is predominantly unaffected by wind erosion and stays within the field, the finer fractions are eroded and blown out (Kok et al., 2012; Shao, 2008). Fine-textured soils favor aggregation and prevent erosion, but the very fine sand fraction is the size with the lowest threshold (Shao, 2008), which can initiate suspension by abrading larger aggregates (Zobeck and Van Pelt, 2015). Overall, wind erosion can redistribute not only soil but also organic carbon (Gregorich et al., 1998). Investigating the wind-blown sediments' composition and the soil organic carbon (SOC) content is a relevant research topic (Iturri and Buschiazzo, 2023). On a local scale, land use sustainability relies on preserving SOC (Shao et al., 2011). Globally, unknown SOC rates of aeolian sediments from semi-arid environments cause uncertainty in carbon cycle estimates (Chappell et al., 2013).

Wind tunnel experiments have been used to understand the combined effects of topsoil characteristics and agricultural management practices influencing surface characteristics and soil loss rates. Sirjani et al. (2019) and Shahabinejad et al. (2019) showed a significant relationship between soil erosion rates and the mean weight diameter in Iran's arid and semi-arid regions. Overall, various studies show the significant effect of tillage on soil structure (Bronick and Lal, 2005) and the associated increase in erosion risks (Zobeck and Popham, 1990). After studying the aerodynamic roughness of five cultivated soils, Zhang et al. (2004) concluded that roughness length is the dominant parameter in evaluating soil erodibility on arable soils in China. It is well known that the soils erodibility of fixed sandy soils can accelerate under cultivation (Li et al., 2004; López et al., 1998; Reynolds et al., 2007). However, on-farm experiments that measure soil losses caused by wind erosion after the application of mechanical stresses are limited.

We provide the first indications from in situ measurements for the control and prevention of wind erosion on arable land in Central Asia's dry steppe. A mobile wind tunnel was used to explore the erosion risk of different surface characteristics under the natural conditions of Kazakhstan's agricultural steppe soils. We examined short-term soil and SOC loss as well as changes in soil characteristics at a field scale caused by aeolian processes in response to different management practices commonly used in agriculture. Wind tunnel experiments were conducted after recent steppe conversion on a bare and cloddy surface and further cultivated and sown with barley and maize. Additional experiments were conducted after applying different mechanical stresses to evaluate the effect on soil loss. Mechanical disruptions were comparable to the forces soils experience under real conditions during field cultivation. Therefore, aggregate breakdown by a light cultivator and a disc harrow was imitated by hand with a lifting or a turning tool. The pulverizing effect of aggregates by heavy tillage implements on tractor tire tracks was simulated by crushing aggregates intensively. To verify the functionality of the mobile wind tunnel, we compared the aeolian sediments collected during the experiments inside the tunnel and aeolian deposition from natural wind erosion events.

The main objectives of this study are (i) to quantify soil losses depending on different agricultural management practices and surface characteristics, (ii) to determine the changes in particle size distribution (PSD) and aggregate size distribution (ASD) of aeolian sediments and depositions, and (iii) to quantify SOC losses due to wind erosion.

2. Materials and methods

2.1. Study area and test site

The study area is located in the Eurasian steppe in northern Kazakhstan. The test site is located east of Astana and north of Pavlodar (Fig. 1A). The area of interest has been shaped by floodplains of the Irtysh River or lacustrine-alluvial depositions from thermokarst lakes during the Quaternary (Aubekerov and Gorbunov, 1999). The soils at the test site were assigned to Haplic Kastanozem (FAO, 2014) and Chestnut in the national classification system (Stolbovoi, 2000). The nearby Irtysh River has the highest water security in Kazakhstan and can be used for irrigation (FAO, 2012). Overall, the fertile soils favor the cultivation of cereals in northern Kazakhstan, but climate conditions cause a permanent risk of wind erosion (Fig. 1B).

The climate is dry continental, with an annual mean temperature of 2.9 °C and annual precipitation of 299 mm at 2 m height (based on weighted interpolation 1991–2020) (Harris et al., 2020; Zepner et al.,

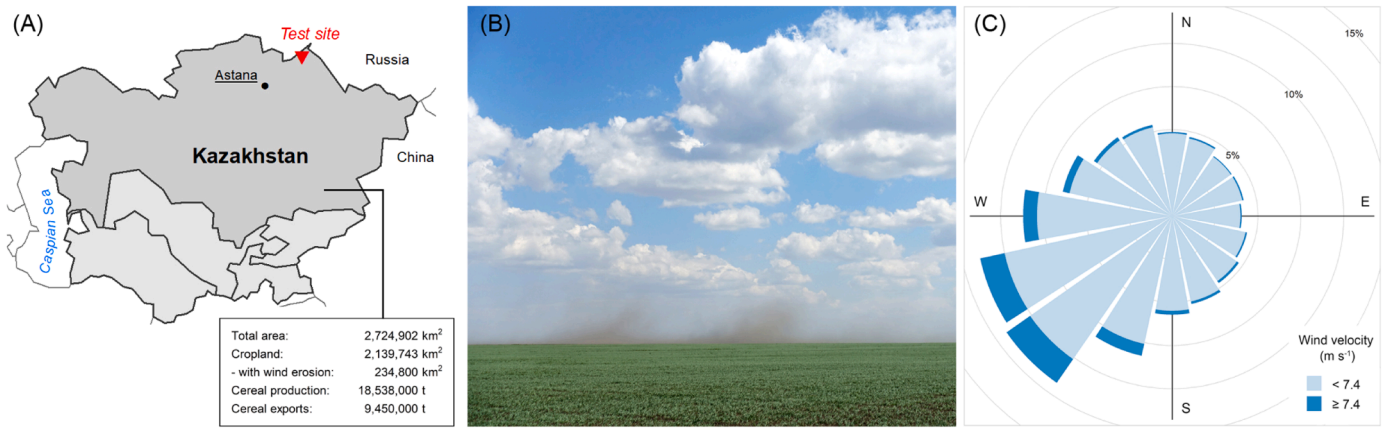

Fig. 1. Location of the test site in northern Kazakhstan (A). Typical agricultural environment in the dry steppe of Kazakhstan with aeolian sediments moved by suspension during a common wind erosion event observed on the test site in June 2022 (B). Relative frequency (%) of wind velocities, classified for 16 wind directions (average of 1991–2020). Wind speeds (at 10 m height) below (light blue) and above a threshold of 7.4 m s^{-1} (dark blue) are shown (C).

2021). Wind is always present in the study area with the highest speed in winter and spring. The average mean wind speed in the study area at a height of 10 m is 4.1 m s^{-1}, with strong wind gusts exceeding 40 m s^{-1}. The main wind direction is southwest (Fig. 1C) (DTU, 2021; FAO, 2012; Meteoblue, 2023). The estimated threshold wind speed is 4 m s^{-1} at 0.3 m height (Scheffer et al., 2016), corresponding to 7.4 m s^{-1} at 10 m height derived from the logarithmic wind profile (Shao, 2008; Wieringa, 1992). The transport capacity Q (dimensionless) of the wind (Fig. 2) can be calculated based on the Eq. 1:

$$Q = u^2(u - u_t) \quad (1)$$

where u (m s^{-1}) is the wind speed and u_t (m s^{-1}) is the threshold wind speed (Fryrear et al., 1998; Funk et al., 2023).

Three adjoining agricultural fields (140 ha each) were used for the experiments. They had been abandoned for several years and were covered with typical grassland vegetation (locally called *zalesh*). One field represents the primary situation, as the conversion from grassland steppe to arable land was carried out before by breaking the grass cover with a disc harrow and stirring the soil up to 0.25 m depth with a cultivator in the spring of 2022 (Plot 1). As usual, cultivation with a crop did not follow immediately, and the initial surface remained fallow in a rough, cloddy state. The two arable fields share the same history. They were converted from steppe in 2019 by disc harrow and cultivator. The fields were cultivated with barley in 2020, with potatoes in 2021, and seedbed preparation was carried out on both arable fields with a cultivator (depth of 0.2 m) in May 2022. Afterward, one field was sown to barley (Plot 2) and the other to maize (Plot 3). Both are common crops in the study area.

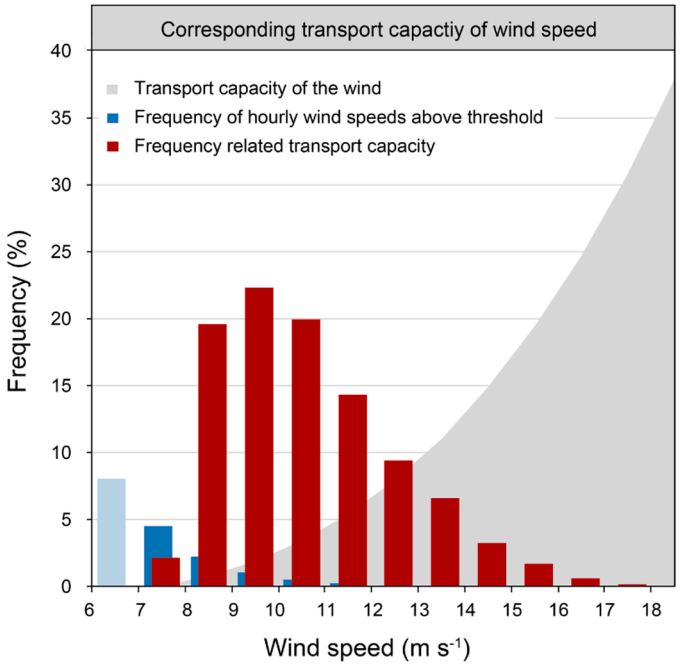

Fig. 2. The transport capacity of the wind (gray area), the frequency of hourly wind speeds above a threshold of 7.4 m s^{-1} (blue bars), and the frequency-related transport capacity (red bars) of the test site are shown.

2.2. On-farm experimentation

2.2.1. Design

On-farm experiments are challenged by ensuring plot uniformity and remaining other factors equal while isolating the consequence of mechanical stress (ceteris paribus effect). Nevertheless, they are of unique value and of great expressiveness that comes from conducting experiments under real farm management conditions. This on-farm experiment was designed to study wind erosion processes and quantify soil losses under typical conditions in agriculture (Fig. 3). The experiments were conducted with a mobile wind tunnel, which allows repeated investigations of aeolian processes within a shorter time than in the natural environment, where these factors are highly variable in time and space (Van Pelt and Zobeck, 2013). Wind tunnel measurements were conducted in June 2022 when plants had just emerged, but soil surfaces were still susceptible to wind erosion. This allowed us to study wind erosion at the transition from bare soils to early stages of plant development. Surfaces were prepared as tilled with a cultivator, disc harrow, or pulverized by tractor tires. The timing of the experiment also ensured that they were conducted under climatic conditions where soil loss by wind erosion occurs regularly in the study area (FAO, 2012).

2.2.2. Setup: mobile wind tunnel

The mobile boundary layer wind tunnel shown in Fig. 4A (Umwelt-Geräte-Technik GmbH, Müncheberg, Germany) was extensively tested under various conditions to become familiar with its technical characteristics before conducting experiments. An axial fan of 7.7 kW powered the air stream of the push-type tunnel. In the field, the electric power was provided by an 11.5 kW diesel generator. The fan and generator are mounted on a two-axle trailer. A 5-m long flexible hose leads the air stream to a flow straightener on the ground, eliminating the fan's vortexes and ensuring a laminar flow. The flow straightener consists of PVC

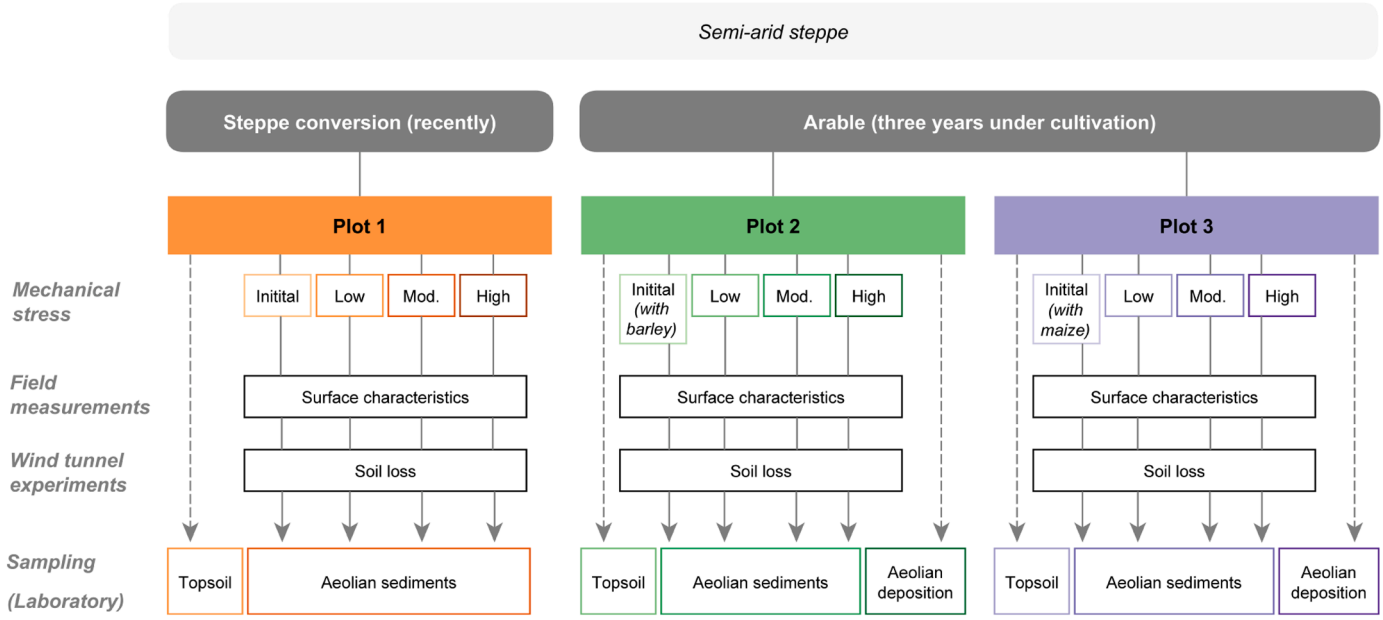

Fig. 3. Hierarchical data structure defining the study design.

Fig. 4. The mobile wind tunnel during experiments on maize (A), MWACs and SUSTRA for collecting aeolian sediments at the wind tunnel outlet (B), and aeolian depositions from natural wind erosion events on the edge of a field (C).

tubes (length = 150 mm, diameter = 12 mm, material thickness = 0.23 mm) and has the same cross section as the measurement section (height = 0.8 m, width = 0.8 m). The measurement section consists of six single segments (total length = 6 m) placed on two metal rails over an open surface area of 4.8 m^2. Each segment has an acrylic glass window, allowing visual observation and easy access to the inside of the tunnel between measurements. The power supply for the fan is adjustable by an attached control panel for a regulated increase in wind speed. A cup anemometer at the end of the tunnel at the height of 0.5 m was used to monitor comparability between all experiments independent of ambient conditions (temperature, air pressure, wind speed, wind direction) on the test site.

The air stream of the mobile wind tunnel showed a logarithmic wind speed profile up to 0.4 m height measured on raw concrete, comparable to sandy roughness (Appendix Fig. A1A). A maximum wind speed of 16 m s^{-1} was measured at 50 Hz (u^* = 0.85 m s^{-1}). Wind profiles of the roughness lengths of this study are presented in Appendix Fig. A1B. To ensure that the simulation of saltation in the wind tunnel is comparable to the development under natural conditions, the Froude number criterion was used (White and Mounla, 1991). The Froude number F (dimensionless) value can be calculated with Eq. 2:

$$F = \frac{u^2}{gH} \tag{2}$$

where u (m s^{-1}) is the uniform wind tunnel speed, g (m s^{-1}) is the gravity constant, and H (m) is the restricted height of the wind tunnel. The saltating flow in the wind tunnel is free of facility constraints below a value of F = 20 (Owen and Gillette, 1985, as cited in White and Mounla, 1991) or below the more conservative value of F = 10 (White and Mounla, 1991). The dimensions of this mobile wind tunnel allow a Froude number of 20 at 12.5 m s^{-1} or 29 at 15 m s^{-1} speed. However, the ideal Froude number can usually only be archived in large stationary wind tunnels at very low wind speeds (Maurer et al., 2006).

2.2.3. Setup: sediment traps

Two types of passive sediment traps were used at the end of the wind tunnel to collect eroded material (Fig. 4B). Modified Wilson and Cook (MWAC) samplers were used to measure the vertical distribution of the aeolian sediments. The MWAC consists of a PE bottle of 100 ml and a glass in- and outlet tube with an inner diameter of 8 mm. They were installed at the ground level and attached to a pole at 0.05 m, 0.10 m, 0.15 m, 0.20 m, 0.25 m, 0.30 m, and 0.35 m height to collect eroded material. The MWAC samplers are popular in wind erosion studies and seem less influenced by ambient wind speed (Zobeck et al., 2003). Since very low collection rates were possibly to be expected, MWACs of all heights were weighed before and after each experiment. Additionally, a SUSTRA (Suspension Sediment Trap, replica by Umwelt-Geräte-Technik GmbH, Müncheberg, Germany) with an opening diameter of 0.05 m was used to collect sediments in the height range between 0.025 and 0.075 m (Funk et al., 2004; Funk and Engel, 2015; Janssen and Tetzlaff, 1991) to catch higher amounts of aeolian sediments for further analyses. The traps were installed in the center of the tunnel with space to each other to keep the air stream's disturbance as low as possible.

The vertical distribution of the horizontal sediment loss was used to

quantify wind erosion (Funk et al., 2014). Therefore, the sediment mass collected in the MWAC was related to the MWAC's inlet surface area of 2.655×10^{-4} m^2 and the surface area inside the mobile wind tunnel. Then, the soil loss (g m^{-2}) was derived from semi-logarithmic regression by fitting the total mass of caught sediments (q_z) at the height (z) to ln(z) (Koza et al., 2023). Quantifying soil loss with the MWACs allows good repeatability. An experiment with five repetitions on a highly erodible surface showed a standard deviation of 8.8%.

The SOC ratios were calculated as the content of SOC collected by the traps to the content of SOC in the topsoil.

2.2.4. Procedure

The weather conditions were comparable during the entire time of investigations. The mobile wind tunnel was aligned in the same direction as the crop rows, which were also aligned with the main wind direction in the study area. All experiments were conducted consistently. The wind speed was steadily increased within the first 5 min from 0 m s^{-1} to 15 m s^{-1} (at 0.5 m height) and held constant for an additional 55 min. Various experiments with running times up to 120 min were conducted before ensuring the soil loss was completely depleted during each experiment independent from plot or mechanical stress applied. Hence, the maximal soil loss was measured for each individual experiment.

The mobile wind tunnel simulated wind erosion events on three experimental plots. Plot 1 had a bare surface after steppe conversion in preparation for fallow. Small plant residues and clods were left from the land cover change (Fig. 5A). In contrast, emerging plants from the previous seeding covered the arable plots (Plot 2 and Plot 3). Barley (*Hordeum vulgare L.*) was grown on Plot 2, and maize (*Zea mays L.*) on Plot 3. Plant heights were comparable (0.15 m) but differed in densities and plant silhouettes. Barley had eight tillers (BBCH code 28) on average at the current phenological stage of development, and maize plants had four unfolded leaves (BBCH code 14) (Meier, 2018). The barley field was covered with 200 plants per m^2 and a row distance of 0.18 m. The maize field was covered with eight plants per m^2 with a row distance of 0.7 m and a distance between plants of 0.1–0.2 m. However, while Plot 2 had weak crusted soil (Fig. 5B), topsoil material on Plot 3 had already been pre-sorted (Fig. 5C) due to previous natural wind erosion events. Thus, there were already deposits in the slightly deeper seed rows, which were then easily mobilized again during the wind tunnel experiments, which were orientated along the rows.

Each plot was prepared in four ways before using the wind tunnel. The initial experiment was conducted on the original surface with the undisturbed surface structure and existing plants. The following experiment was conducted at the same position after removing the plants and refreshing and mixing the surface with a small hand-operated rake (three spikes with a length of 60 mm as a lifting tool). Hence, a low mechanical stress as made by a light cultivator was applied. We used the low mechanical stress application as a benchmark for comparing plots and applied stresses, because the initial situation differed in various interfering factors such as soil structure and plant cover. A third experiment at the same position was prepared using a tool with three rotating spikes (radius of 70 mm as a turning tool) applying moderate stress with a disc harrow characterized by further breakdown of the aggregates. Finally, the fourth experiment was conducted at the same place after crushing all aggregates, similar to the pulverizing effect on tractor tire tracks or driving paths in the field.

2.3. Soil analyses

2.3.1. Topsoil and surface parameters

Topsoil samples for physical and chemical analyses were collected in each plot before the experiments from 0 to 25 mm depth using a flat square-cornered shovel (Larney, 2007). The topsoil's PSD was measured with a laser diffraction analyzer (Helos/KR+Quixel, Sympatec GmbH, Clausthal Zellerfeld, Germany). Before laser diffraction, 10 g soil was chemically pretreated with 30% hydrogen peroxide (H_2O_2) to oxidize organic binding material (Koza et al., 2021). In order to complete dispersion for texture analyses, 3 g of soil was pretreated with 0.05 M sodium pyrophosphate ($Na_4P_2O_7 \times 10\ H_2O$) and physically dispersed for 60 s with 60 W sonication. Particle size classes of clay (0–2 μm), silt (2–50 μm), and sand (50–2000 μm) were used to assign soil texture. Subclasses were used for further distinction (Soil Science Division Staff, 2017). Topsoils on all plots were identified as loamy sands (Soil Science Division Staff, 2017). However, while contents of sand, silt and clay were identical on Plot 1 and Plot 2 (sand: 76%, silt:18%, clay: 6%), the sand content on Plot 3 was slightly higher (sand: 83%, silt: 13%, clay: 4%). The pH of 6.5 ± 0.2 (mean ± standard deviation) and electrical conductivity of 137.3 ± 57 μS cm^{-1} were measured in distilled water at a 1-to-2.5 soil-to-solution (weight-to-volume) ratio. Total carbon was analyzed by dry combustion of 1 g of soil at 1130 °C (varioMax Cube, Elementar Analysensysteme GmbH, Langenselbold, Germany). Total inorganic carbon was analyzed by dispersing 2 g of ground sample material in 50 ml 2 M HCl at 50 °C and subsequently detecting the released CO_2 (soliTIC module interfaced to the varioMax Cube). The total carbon content of 15.5 ± 1.7 g kg^{-1} corresponds to the SOC because the inorganic part is negligible (0.1 ± 0.0 g kg^{-1}). The SOC content was slightly higher on the recently converted plot (Plot 1: 17.8 g kg^{-1}) compared to the arable plots (Plot 2: 14.9 g kg^{-1}, Plot 3: 13.8 g kg^{-1}). The gravimetric method determined soil water content (Gardner, 2018). Three samples were collected from each experimental plot and oven-dried at 105 °C for 24 h. The water content was calculated by the difference in sample mass before and after drying and was comparable between all runs (2.2 ± 0.6%).

Erodible fraction (EF) was determined by the dry sieving method. About 1 kg of dry topsoil was collected before each experiment. The EF can be calculated as the weight percent of aggregates < 0.84 mm after separating fragments (Chepil, 1962). In this study, a horizontal dry-sieve

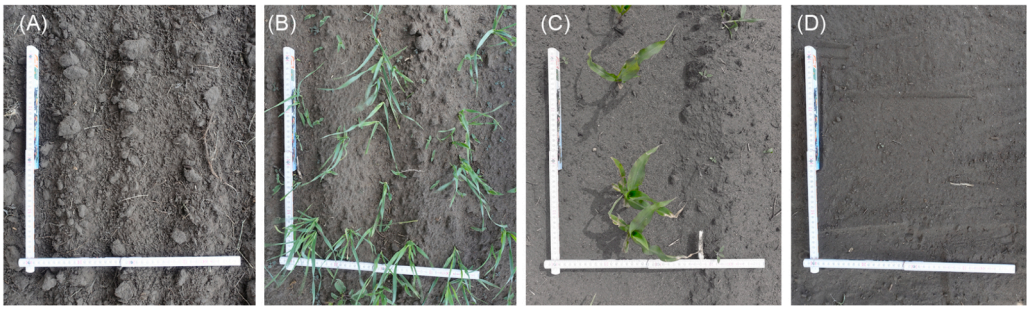

Fig. 5. The initial surface roughnesses: rough cloddy seedbed after steppe conversion on Plot 1 (A), a weak crust on Plot 2 grown with barley (B), and loose material in the rows of maize on Plot 3 (C). The surface roughness without plants and after applying high mechanical stress on Plot 3 (D). The folding ruler is 0.4 m × 0.4 m, showing an area of 0.16 m^2.

(López et al., 2007) with 0.85-mm openings (Koza et al., 2022) was used to calculate *EF* (%) with Eq. 3:

$$EF = \frac{W < 0.85}{TW} \times 100\% \quad (3)$$

where $W < 0.85$ is the weight (g) of < 0.85-mm aggregates and *TW* is the initial weight (g) of the total sample. The risk of wind erosion is considered relatively high for soils with EF > 60% (Larney, 2007) and negligible for soils with EF < 40% (Chepil, 1953). The highest EF of the undisturbed topsoil was measured on the plot cultivated with maize (80.5%), the second highest on the plot cultivated with barley (68.4%), and the lowest after steppe conversion (54.8%). All three plots showed comparable EFs after applying high mechanical stress (83.5 ± 1.1%).

The aerodynamic roughness length (z_0) of each surface was derived as a mean from wind profile measurements with a hot-wire anemometer at three wind speeds. The roughness length of the surface can be calculated based on the logarithmic wind profile with Eq. 4:

$$u = \frac{u^*}{k} \ln\left(\frac{z-d}{z_0}\right) \quad (4)$$

where u is wind speed (m s^{-1}) at height z (m), u^* is the friction velocity (m s^{-1}), d is the displacement height, and k is the Kármán constant (~0.4). Soil roughness length was initially highest on the barley with 8.08 mm (Fig. 5B), second highest after steppe conversion with 7.40 mm (Fig. 5A), and lowest on maize with 5.17 mm (Fig. 5C). After high mechanical stress was applied, the roughness length was initially 0.20 mm on Plot 1, 0.19 mm on Plot 2, and 0.05 mm on Plot 3 (Fig. 5D). Topsoil and surface characteristics of laboratory and field measurements are presented in Table 1.

2.3.2. Aeolian sediments and depositions

Aeolian sediments collected during wind tunnel experiments were also analyzed with laser diffraction, but in combination with a dry dispersion unit (Helos/KR+Rodos Vibri/L, Sympatec GmbH, Clausthal Zellerfeld, Germany. This configuration determines the dry soil's ASD of 2 g in a free aerosol jet, measuring 29 physical classes up to 2 mm. The aggregate size classes microaggregates (<250 μm) and macroaggregates (>250 μm) were derived from the standard hierarchical aggregate order (Tisdall and Oades, 1982). Additionally, typical fractions of different modes of motion during wind erosion events were used for a better classification of aeolian sediments. These are long-term suspension (<20 μm), short-term suspension (20–70 μm), modified saltation (70–100 μm), saltation (70–500 μm) and creep (>500 μm) (Funk and Reuter, 2006; Kok et al., 2012; Shao, 2008).

Sediments collected by the MWACs at the ground level, 0.05 m and 0.10–0.35 m were also analyzed for SOC. Sediments collected by the SUSTRA were analyzed for pH, electrical conductivity, total carbon, total inorganic carbon, PSD, and ASD.

Aeolian depositions from natural wind erosion events in May 2022 were collected from the edges of both arable fields (Fig. 4C) by sampling the layer of buried vegetation (Larionov, 1993). They were analyzed equally to the topsoil and aeolian sediments described above for pH, electrical conductivity, total carbon, total inorganic carbon, PSD, and ASD.

2.4. Statistical analyses

RStudio (Version 4.1.2., RStudio Team) was used for statistical analyses and graphs (R Core Team, 2020). The Shapiro-Wilk test and histograms were applied to test all data for normal distribution. Consequently, the Spearman correlation (r_s) was performed between calculated sediment losses and all measured parameters. A correlation matrix was generated with "corrplot" (Taiyun and Simko, 2021), indicating the significance of correlations at a level of $p < 0.05$. The Randomized Complete Block Design was used to compare different

Table 1
Soil losses from three different plots with similar topsoil and different surface characteristics caused by different mechanical stresses similar to the disruptive forces soil experiences from a light cultivator (low), disc harrow (moderate), and tractor tires (high).

	Plot	Mechanical stress	Topsoil characteristics							Surface characteristics		Soil losses	
			pH	Electrical conductivity	Soil organic carbon	Clay	Silt	Sand	Soil moisture	Erodible fraction	Roughness length	Total	Relative
			(-)	(μS cm^{-1})	(g kg^{-1})	(%)	(%)	(%)	(%)	(%)	(mm)	(g m^{-2})	(%)
Steppe conversion	1	Initital	6.6	72	17.8	6	18	76	1.8	55	7.40	11.7	55
		Low								56	5.21	21.4	(100)
		Moderate								67	5.29	27.1	127
		High								82	0.20	1230.3	5746
Arable	2	Initital *(with barley)*	6.6	129	14.9	6	18	76	3.0	68	8.08	33.8	14
		Low								71	3.80	245.6	(100)
		Moderate								61	5.36	617.1	251
		High								84	0.19	1761.0	717
	3	Initital *(with maize)*	6.1	211	13.8	4	13	83	1.7	80	5.17	1609.0	492
		Low								83	2.34	327.1	(100)
		Moderate								74	2.90	519.3	159
		High								85	0.05	5309.1	1623

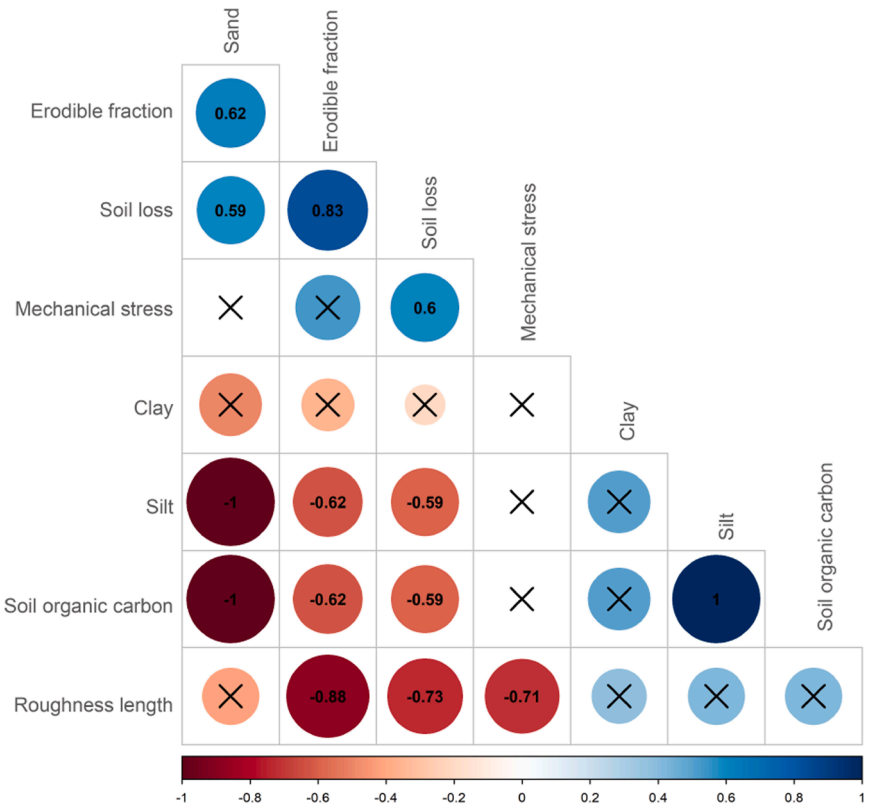

Fig. 6. Correlation matrix shows significant correlations ($p < 0.05$) between soil loss and topsoil and surface characteristics. The strongest correlations between soil loss, erodible fraction, and roughness length are revealed.

mechanical stresses. Each level of stress was replicated on three plots. Statistically, the Kruskal-Wallis test was applied due to rank-based simulations. The Dunn's test was used to identify mean group values that are significantly different ($p \leq 0.1$).

3. Results

3.1. Relationship between soil losses and soil parameters

The results show significant correlations between soil loss, topsoil

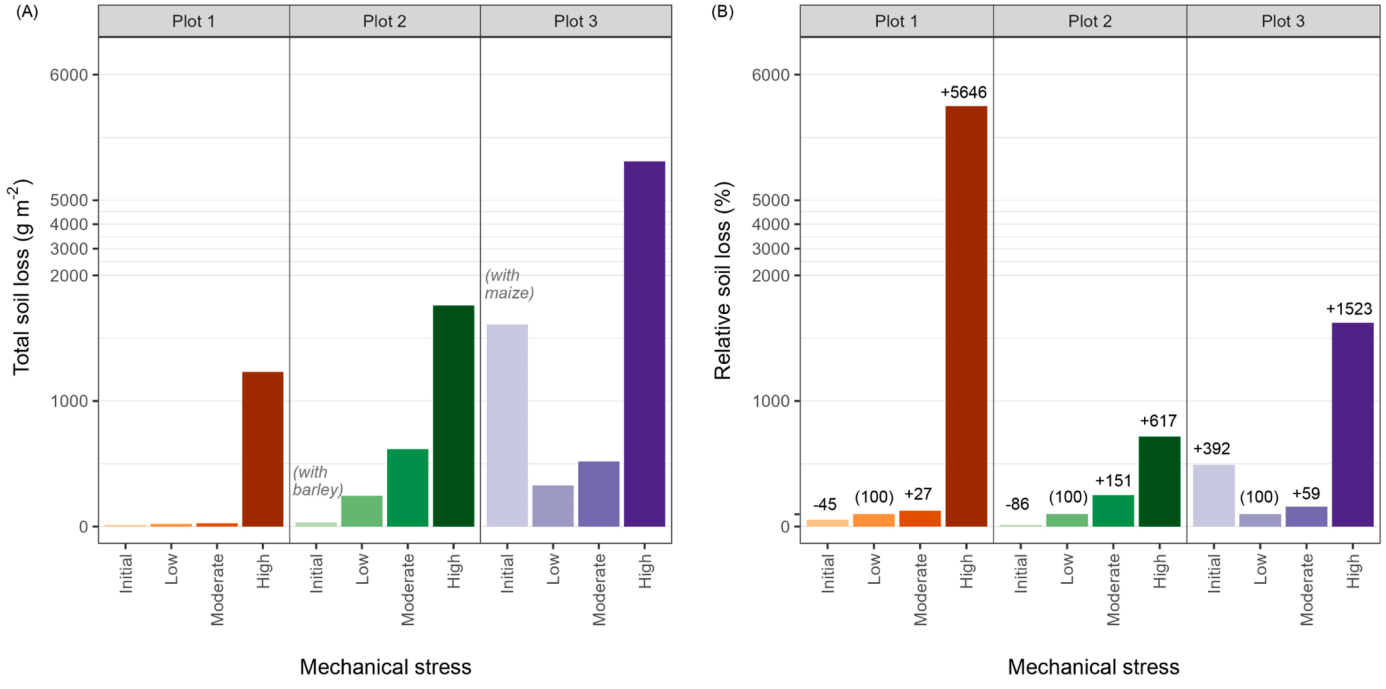

Fig. 7. Total (A) and relative (B) soil loss derived from wind tunnel experiments on three test plots with the initial situation and after different mechanical stresses were applied. During the early growth stages of maize, the soil loss is higher than on the bare surface. Please beware of the compressed scale.

and surface characteristics. The strongest correlations occurred between soil loss, EF, and roughness length. The Spearman rank coefficient analysis showed a strong correlation between soil loss and EF ($r_s = 0.83$), sand ($r_s = 0.62$), as well as mechanical stress ($r_s = 0.60$). The strongest significant negative correlation was observed between soil loss and roughness length ($r_s = 0.73$) as well as silt ($r_s = 0.59$) and SOC ($r_s = 0.59$). Because parent material on the test site did not change between different experimental runs, there was consequently no correlation between applied mechanical stresses and topsoil texture characteristics (Fig. 6).

3.2. Quantity of soil losses

The wind tunnel experiments showed great differences, already under the initial situations. The lowest soil losses were measured on the rough surface after the conversion of steppe to arable land (11.7 g m^{-2}) and on the weak-crusted and well-covered surface of barley (33.8 g m^{-2}). The highest soil loss was measured on maize (1609.0 g m^{-2}), although plants were also present on the surface.

Soil losses significantly differed between the low and high mechanical stress applications. Overall, increasing mechanical stress by tillage or tractor tires increased total soil losses on all three plots considerably (Fig. 7A). The absolute soil losses after tractor tire crushing on Plot 1 (1230.3 g m^{-2}) and Plot 2 (1761.0 g m^{-2}) were in a similar range, which has the same texture but small differences in SOC. Soil loss on Plot 3 was several times higher (5309.1 g m^{-2}), where the highest sand content and lowest SOC are present. Regarding the cultivated area, tractor tire tracks only partially affect agricultural fields. Tillage tools for cultivating barley and maize have a working width of six meters. The tractor's two rear tires have a total width of 1.42 m. Hence, about 23% of each field is disrupted by high mechanical stress that can pulverize aggregates. From this field-size perspective, the relative changes in soil losses between low and high mechanical stress application showed that the application of tillage creates soil structures susceptible to wind erosion, but tractor tires increase soil losses by multiple (Fig. 7B).

With an estimated bulk density of 1.3 g cm^{-3} on the test site, the simulated wind erosion event would cause a loss of topsoil depth of 0.01 mm after steppe conversion and 0.03–1.24 mm after further tillage implementations. On tractor tire tracks, which account for about one-fourth of the fields, 0.95 mm of topsoil would be eroded on Plot 1, 1.35 mm on Plot 2, and 4.08 mm on Plot 3.

3.3. Changes in particle and aggregate size distributions

The PSD of topsoil and aeolian sediments from all plots showed that soils are both bimodal distributed. The two maxima were 7.5 µm and 210.0 µm in particle size. Fine silt (2–20 µm) is up to 14%, coarse silt is below 5%, and very fine sand (50–100 µm) is up to 16%. The fine to medium sand particles (100–500 µm) are the dominant particle sizes with at least 57% (Fig. 8). Comparing the particle size classes of clay, silt, and sand from the topsoil and the aeolian sediments showed a tendency to more finer particles in the sediments of the steppe conservation plot, already beginning in the clay fraction (Fig. 8A, Appendix Table A1). On Plot 2 and 3, aeolian sediments had lower silt and very fine sand content but much higher fine and medium sand fractions (100–500 µm) than the topsoil (Fig. 8B, Appendix Table A1). The fine and medium sand subclasses together showed a relative increase of 31% on Plot 2 (fine and medium sand: topsoil = 54%, aeolian sediments = 71%) and 19% on Plot 3 (fine and medium sand: topsoil = 59%, aeolian sediments = 70%). Plot 1 only showed a relative increase of 4% (fine and medium sand: topsoil = 54%, aeolian sediments = 56%) because of contrary trends within these two subclasses. However, this trend in which fine and medium sand particles' content increases during wind erosion is explicit if PSD from the depositions is considered. The depositions showed a distinct relative increase of the fine and medium sand of 41% for barley (fine and medium sand: deposition = 76%) and 34% for maize (fine and medium sand: deposition = 79%) compared to the topsoil. This also becomes apparent by the increasing slope of the PSD curve for the aeolian sediments. On the contrary, particles below 100 µm decrease in the aeolian sediments, especially the fine silt fraction. In general, results showed no major change in clay particles. Coarse sand particles (500–100 µm) get detached only occasionally and are less than 1% in the depositions.

Results of aggregate size analysis showed that independent of the samplers's height, aeolian sediments contained mainly (65–86%) microaggregates (<250 µm) and some (14–35%) macroaggregates (>250 µm). Non-erodible aggregates larger than 850 µm were collected only in negligible amounts (Fig. 9). Even though differences in ASD at ground level and 0.05 m height were minimal, the percentage of microaggregates decreased with increasing height. Aggregates suitable for typical long-term suspension (<20 µm) were collected on the steppe conversion plot (2–4%) but only marginally on the arable plots. Comparing aeolian sediments at the ground level with sediments from 0.10 to 0.30 m height showed that aggregates suitable for short-term suspension increased on Plot 1 with height (19–29%), but decreased on Plot 2 (13–6%) and Plot 3 (12–9%) (Appendix Table A2). At the same

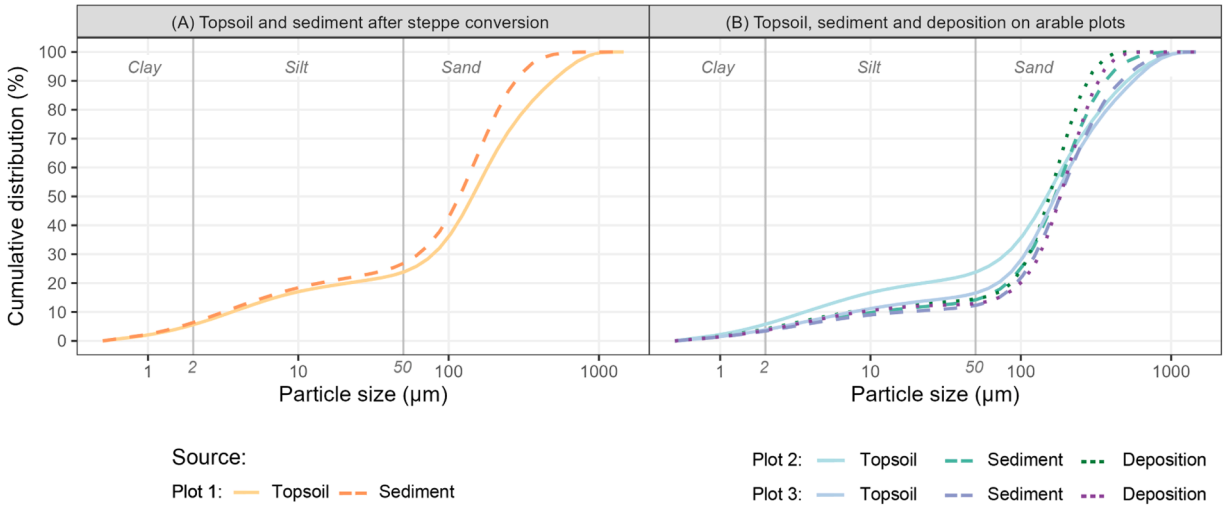

Fig. 8. Particle size distribution from topsoils (solid line), aeolian sediments collected during wind tunnel experiments (dashed line) by SUSTRA, and depositions from natural wind erosion events (dotted line).

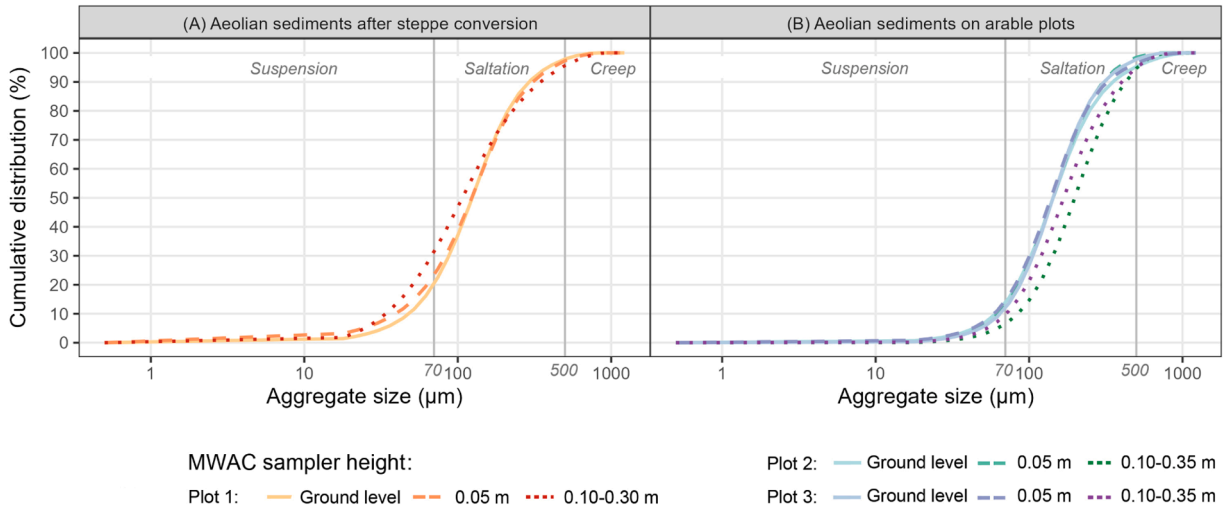

Fig. 9. Aggregate size distribution from aeolian sediments collected during wind tunnel experiments by MWAC samplers at the ground level (solid line), 0.05 m (dashed line), and 0.10–0.35 m (dotted line) during wind tunnel experiments.

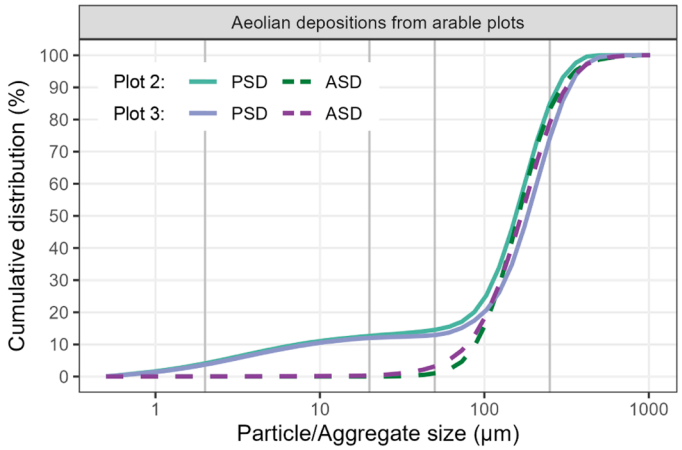

Fig. 10. Comparison of the particle (solid line) and aggregate (dashed line) size distribution of aeolian depositions from natural wind erosion events on arable plots.

time, the aggregate fraction typical for saltation changed contrary. They decreased on Plot 1 (78–64%) (Fig. 9A) and increased on Plot 2 (81–88%) or remained at a high level on Plot 3 (86–85%) (Fig. 9B). While aeolian sediments collected from arable plots above 0.05 m height were larger in size than sediments collected near the ground, this applied for only for 20% of the distribution from the steppe conversion plot (crossing point between solid and dashed/dotted line in Fig. 9A).

Comparing particle and aggregate size analyses from aeolian depositions revealed that PSD is bimodal while aggregates are unimodally distributed. However, there is no major difference for about 80% of the distribution. Independent of the method, particles and aggregates above 100 µm were similarly distributed. In contrast, size distributions showed that depositions contain about 20% of particles < 50 µm and 10% of particles < 20 µm while aggregates < 50 µm are rare and aggregates < 20 µm are negligible (Fig. 10).

3.4. Quantity of soil organic carbon losses

The SOC content in the topsoil was slightly higher on the steppe conversion plot compared to arable Plots 2 and 3. Comparing the SOC contents of topsoil and aeolian sediments from all plots revealed major differences between the steppe conversion plot and the arable plots. While there was a SOC increase of 69% in the aeolian sediments compared to the topsoil on Plot 1, there was a decrease of 13% on Plot 2 and a decrease of 35% on Plot 3. The SOC decline was also apparent in the depositions, similar to the PSD results. The depositions showed a decline of SOC in the depositions of 22% on Plot 2% and 36% on Plot 3 (Fig. 11, Appendix Table A3). The calculated soil loss and the SOC content of the aeolian sediments could be used to estimate the total losses of organic carbon. The loss of SOC mass was estimated to be 0.3 g m^{-2} on the steppe conversion plot, 0.4 g m^{-2} on Plot 2, and 14.3 g m^{-2} on Plot 3. However, after high mechanical stress, the total organic carbon loss on Plot 1 with 36.9 g m^{-2} was higher than Plot 2 with 22.8 g m^{-2}, even though higher total soil loss was recorded. Similar to the total soil loss, the mass loss of organic carbon was highest on Plot 3 with 47.3 g m^{-2}.

The ratio of the SOC content collected by MWACs at different heights showed no variation between ground level and near-ground (0.05 m height). Still, the SOC ratio was enriched in aeolian sediments collected at a sampler height of 0.18 m on the steppe conversion plot and depleted on the arable plots at 0.20 m height. The contrary trends between the steppe conversion and arable plots are visualized in Fig. 12. Soil organic loss was further proven by observing depletions in the aeolian depositions of Plot 2 (SOC ratio = 0.78) and Plot 3 (SOC ratio = 0.64) (Fig. 12, Appendix Table A3).

4. Discussion

4.1. Influence of topsoil and surface on soil erodibility

Significant relationships between EF and roughness length, as well as mechanical stress and roughness length, prove that the interactions between properties affect wind soil erodibility. On the test site, EF and roughness length have the greatest effect on soil loss. This finding aligns well with previous studies by Zhang et al. (2004), Sirjani et al. (2019) and Shahabinejad et al. (2019). Altogether, our results reinforce the importance of ASD and linked roughness length to the soil's susceptibility. Recent studies showed that soil aggregation in northern Kazakhstan depends on organic binding material, favored by high amounts of silt and clay particles (Koza et al., 2022, 2021). This also applies to this study's test site, where soil loss increases with decreasing silt and SOC content. Nevertheless, the typical amount of SOC on the test site is comparable with results from sandy soils worldwide (Yost and Hartemink, 2019). Thus, the sandy soils of the Kazakh Steppe can be easily incorporated into models or evaluation schemes of erodibility.

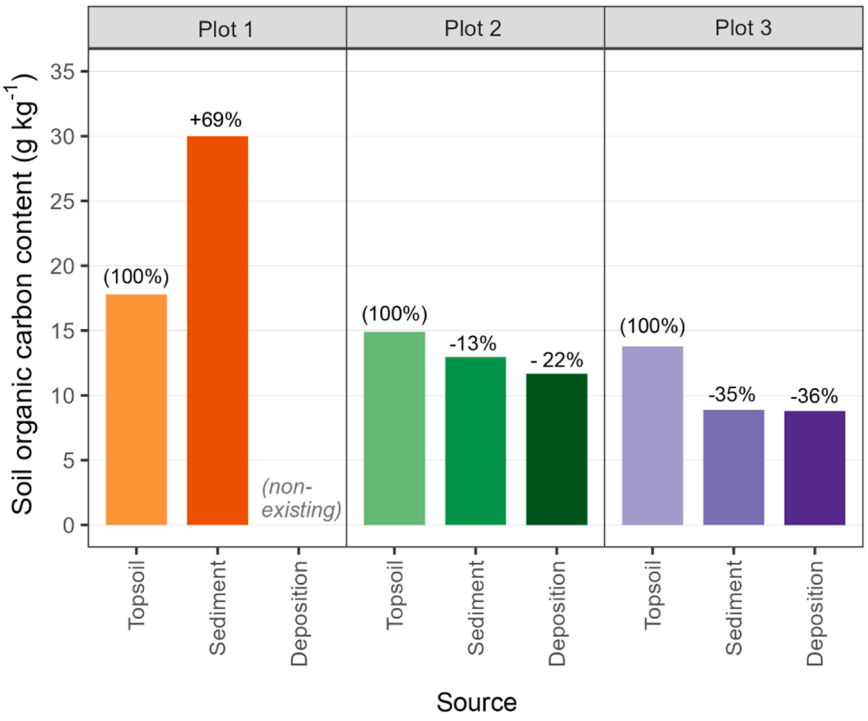

Fig. 11. Soil organic carbon content from topsoil, aeolian sediments collected during wind tunnel experiments by SUSTRA, and aeolian depositions from natural wind erosion events. Relative organic loss is shown above each bar.

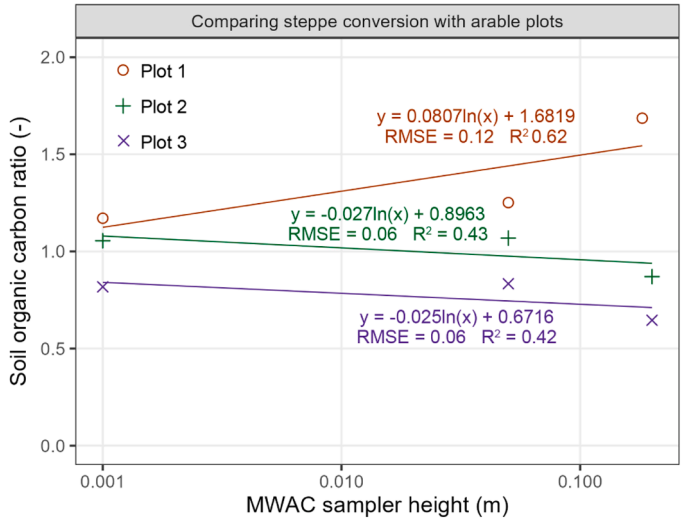

Fig. 12. Comparison of soil organic carbon ratio after steppe conversion (Plot 1) and arable plots (Plot 2 and 3) for different heights. Additionally, trend lines are shown.

4.2. Soil losses by wind erosion

Historical climate data (1991–2020) show that wind speeds above the threshold of 7.4 m s^{-1} occur on average about 6.5% of the year (Fig. 1C). Based on the frequency distribution of wind speeds above 7 m s^{-1} and the corresponding transport capacity of each wind speed, the weighted transport capacity was derived. Frequency-related transport capacity is highest between 8 and 11 m s^{-1} (Fig. 2), accounting for more than 60% of the total loss capacity in the study area. Wind tunnel experiments were conducted with a wind speed of 15 m s^{-1} (at 0.5 m height). Considering the logarithmic wind profile, the wind tunnel simulations are comparable to natural wind speeds above 13.2 m s^{-1} (at 10 m height) on a low roughness length of 0.05 mm. On average (1991–2020), wind speeds exceed 13.2 m s^{-1} for about 6 h per year (Meteoblue, 2023), but account for more than 10% of the frequency-related transport capacity. The overall outcome is consistent with the findings from northeast Germany (Funk et al., 2023). Please note that the mentioned weather data are hourly averages, which underestimate wind erosion because gusts are not considered, or on the contrary, wind erosion is overestimated if soil is covered.

It is well known that sandy soils, which are dominant in the study area, are more susceptible to wind erosion than fine-textured soils (Chepil, 1952). This result aligns with a previous study (Koza et al., 2022) on a test site with loamy sand about 200 km away, where the soil

erodibility was determined from aggregate stability tests. The previous and present studies underline the continuation of the degradation processes by wind erosion in the study area. The wind tunnel itself constraints saltation during simulation because the calculated Froude number is above 20. Therefore, soil losses calculated from the vertical distribution of the mass fluxes in the tunnel provide safe estimates because transport profiles of real events are assumed to increase more with height, resulting in higher transport rates. The lowest soil loss was measured after the recent steppe conversion (Plot 1) on the bare surface. Immediately after converting steppe to arable land, aggregate stability was at its best, and the SOC content was highest. Since it was the first intervention after a long period without tillage, these aggregates still represent a part of the natural soil structure. Clods resulting from steppe conversion were decisive for the high roughness length and an effective measure against wind erosion. With further tillage, these clods are subjected to further breakdown. Similar results were obtained from cultivated fine-textured soils of the semi-arid region of Argentina (Colazo and Buschiazzo, 2010) and northwest China (Zhang et al., 2004). Comparing the effects of vegetation cover of barley and maize showed that the soil loss by wind erosion was highest on maize. Even though both arable plots had soils with EFs above 60%, indicating a high erodibility risk (Larney, 2007), the roughness length was lowest on maize. The relatively low number of plants with high row distances favored wind erosion in this early plant growth stage. With a mobile wind tunnel, Funk and Engel (2015) showed that wind can blow below the plant canopy of maize without considerable resistance throughout different growth stages. Similar results were obtained by Burri et al. (2011) for perennial ryegrass on sand. Our results for maize support the findings that soil losses during early growth stages can be higher than losses on the bare surface. It is also important to remember that soil loss on maize is different between plant rows and close to the plants themselves. Without considering the variability over the wind tunnel width, the shown results are estimations (Dong et al., 2004; Funk and Engel, 2015). For maize, the horizontal distribution of the soil loss across the wind tunnel width is highest close to the plant row and lowest between rows (Funk and Engel, 2015). Therefore, the soil loss on maize is lower if the row orientation is not parallel to the wind. In contrast, soil loss was lower with barley plants compared to the bare surface.

Farming practices can affect susceptibility considerably. The experiments showed that the mechanical disruptions in this study caused higher EFs and lower roughness lengths, accompanied by increased soil loss. Disc harrow (turning and mixing tool) caused higher soil loss than tillage with a light cultivator (lifting tool). Even though we only imitated different tillage practices, the findings agree with the study by Tanner et al. (2016), where real practices were implemented in field experiments. Our results confirm the presumption that mechanical stress by tillage weakens soil structure by breaking down aggregates, leading to increasing erodibility.

Our experiment also proved that crushing soil clods with tractor tires under dry conditions is a key contributor to soil loss from wind erosion. This worst-case scenario for aggregate breakdown is considered an important wind erosion source in the study area. Our results align with a study on Polish loamy sands, in which tractor tires were identified as a major wind erosion source (Podsiadłowski, 1988). An important step in the overall consideration of wind erosion susceptibility will be to incorporate this aspect into the design of cropping systems. Measures that prevent the destruction of dry aggregates include the consideration of soil moisture during agricultural practices, such as the timing of sowing, the temporal variation during the day, and the variability of tillage depth.

This study proves that soil degradation by management is an ongoing challenge in the study area representing semi-arid ecosystems of Central Asia (Robinson, 2016). The main objectives of erosion control are maintaining soil fertility and preventing soil loss rates from exceeding natural soil formation (Larionov, 1993). In Central Asia, conservation agriculture has developed rapidly over the past 15 years, particularly in northern Kazakhstan. Currently, 10.5 million hectares are under reduced tillage, and about 2.5 million hectares (about 15.6%) of cropland are under permanent no-till rotations (Kassam et al., 2019). No-till systems cut through the residues, leaving the soil less exposed to wind or the disruptive forces of saltating particles (Verhulst et al., 2010). In addition, no-till also improves uniform snow depositions, limits evaporation and weed growth, while yields stabilize after several years of consistent implementation (Lafond et al., 2006; Meinel et al., 2014). No-till farming practices could potentially solve the wind erosion problem in semi-arid steppe soils. It is expected that no-till is likely to expand in Asia (Lal et al., 2007) due to the increasing availability of suitable herbicides and high-quality seeding technologies (Grunwald et al., 2016). However, Central Asia's institutional, socioeconomic and agroecological contexts are diverse and require a geographically differentiated approach. In northern Kazakhstan, replacing the common bare summer fallow with cover crops such as legume forages is recommended (Suleimenov et al., 2016). However, supplies for no-till systems are sometimes too expensive for farmers and there is still a need for knowledge regarding the application under semi-arid climatic conditions (e.g., heavy rains in spring make it difficult to apply herbicides successfully). Overall, information on crop management based on conservation agriculture in Central Asia is incomplete (Kienzler et al., 2012). At the test site, strip-till was implemented in 2023 as an adaptation measure after severe soil degradation by wind occurred in 2022.

4.3. Particle and aggregate size distributions of the soil losses

The results of this study show the sorting process caused by wind erosion events on all plots. Noticeably, on the steppe conversion plot, all particles finer than medium sand (<200 μm) are enriched in the aeolian sediments except for clay. In contrast, only the fine and medium sand particles (100–500 μm) are enriched in the aeolian sediments and depositions on the arable plots. In conclusion, relatively more silt particles get eroded on the recently converted field compared to the arable fields that have been under cultivation for three years already. Lackóová et al. (2021) studied the long-term impacts of wind erosion on PSD in a dune region of Slovakia. They showed that fine particles could be eroded within a few years, changing soil texture. Our results indicate that particles below 500 μm are being carried away, causing a shift of the soil texture class into sand. This can also be detected in the results (Fig. 8), where the PSD curve follows a trend towards the typical distribution curve of dune sands with textural particles ranging from 100 μm to 1000 μm (Pye, 1994).

Furthermore, our results of aggregate size analysis from aeolian sediments are within the typical range of saltation. Most aggregates have a size of 70–500 μm, which is in the common saltation fraction (Shao, 2008). Measured aggregate sizes align with various studies showing that mainly mircoaggregates between 20 and 250 μm are depleted by wind (e.g., Yan et al., 2018). This aligns with Zamani and Mahmoodabadi (2013), who suggested that macroaggregates cause the low EF of soil in arid and semi-arid environments. Creeping particles (>500 μm) were only trapped rarely. Aggregates with sizes suitable for long-term (<20 μm) and short-term suspension (20–70 μm) (Shao, 2008) were collected on the steppe conversion plot but only rarely on the arable plots. Still, the aggregate size of each transport mode may vary depending on wind speed, aggregate density, and saltation/creep load change (Hagen, 2001).

Analyzing PSD and ASD of aeolian depositions from natural wind erosion events underlines the results obtained with the wind tunnel experiments. They confirm the functionality of the mobile wind tunnel for imitating real events. The PSD and ASD from aeolian sediments collected during saltating processes are similar to the distribution of the depositions. Comparing PSD and ASD within the depositions reveals no differences for particles > 100 μm, which account for 75–81% of the soil. Hence, fine sand particles and coarser do not aggregate and can saltate several millimeters to several meters along the surface (Shao,

2008). About 19–25% of aggregates in the depositions are between 20 μm and 100 μm. Those aggregates account for all clay and silt particles bound together with organic matter. They are suitable for modified saltation and short-term suspension, typically accounting for several hours in the air while being transported hundreds of kilometers (Shao, 2008).

4.4. Soil organic carbon losses by wind erosion

The results of this study show the selective character of erosion processes, as the clay and silt fractions of the soils contain disproportionately greater amounts of SOC (Chappell et al., 2013; Zobeck and Fryrear, 1986). Comparing topsoil and aeolian sediments revealed enrichment of SOC in the eroded materials. Hence, wind erosion can be one factor responsible for the typical decline in SOC content in the topsoil caused by steppe conversion to arable land. In our recent study, we also observed this decline between grass- and cropland in northern Kazakhstan (Koza et al., 2022), similar to the nearby Kulunda steppe (Bischoff et al., 2016). Still, Gregorich et al. (1998) reviewed that carbon losses by mineralization are dominant within the first years after conversion, and erosion becomes a more important process after establishing a new equilibrium a few years later. From the recently converted plot, fine particles and aggregates suitable for suspension were removed, while on the arable plots, the dominant fractions were in the size range typical of saltation. Aeolian sediments and depositions were not enriched with SOC. The slightly enriched SOC ratio of the steppe conversion plot can be considered a reasonable value for SOC loss from topsoil by suspension and is comparable to various studies (Nerger et al., 2017). In contrast, the ratio of the arable plots is < 1. A loss of SOC is registered but somewhat unusual because SOC ratios in the saltation layer from literature are mainly > 1 (Li et al., 2020a; Nerger et al., 2017). This means that disproportional amounts of SOC do not get removed by saltation on this loamy sand test site. However, the depletion of SOC in the aeolian sediments from arable plots can be easily explained by the higher amount of fine and medium sands in aeolian sediments and depositions, unfavorable for the organic binding material. Zenchelsky et al. (1976) observed that the SOC ratio also depends on the wind speed. High wind speeds (11.4 m s^{-1}) resulted in lower SOC ratios compared to low speeds (7.3 m s^{-1}). Larger soil fractions containing more mineral than organic matter were eroded with increasing speed. This aligns with our experimental setup of 15 m s^{-1} and the archived results.

Therefore, wind erosion does not necessarily lead to a decline in primary productivity on cropland. Still, it is important to consider that the total soil loss was substantially higher on arable plots where aeolian sediments were depleted of SOC, compared to the low soil loss on the steppe conversion plot with the highly SOC-enriched sediments. Hence, estimations revealed that after applying high mechanical stress, the soil loss on the arable plot with the same texture (Plot 2) is higher than on the steppe conversion plot, but the total SOC loss is lower.

5. Conclusions

This study assesses the risk of wind erosion in the semi-arid steppe of Kazakhstan, one of Central Asia's most important regions for growing crops. We show first effects of wind erosion as a soil degradation process based on results obtained from field experiments:

i. Mobile wind tunnel experiments verify that agricultural management practices severely increase the risk of wind erosion on sandy steppe soils in different ways. After the recent steppe conversion, soil loss was low. On arable plots that underwent cultivation during the past three years, soil losses increased considerably. In the early growing season, fields cultivated with barley were less affected by wind erosion than maize fields. Among common agricultural practices, a disc harrow caused higher soil losses than a light cultivator. The most severe soil losses originate from experiments simulating tractor tire tracks or driving paths in the field.
ii. Wind erosion caused sorting processes on all plots. After recent steppe conversion, PSD and ASD of the aeolian sediments showed a composition that indicates a higher susceptibility for suspension transport. At the same time, aeolian sediments and depositions originated from arable plots were generally coarser and in the typical size range of saltation.
iii. Associated with the sorting process of particles and aggregates on the recently converted plot, the suspension-dominated aeolian sediment was enriched in SOC and blown out from the field. In contrast, the saltation processes on the arable plots caused a depletion of SOC in the aeolian sediments and resulted in depositions on the field edges with lower SOC.

Altogether, wind erosion due to steppe conversion is a considerable factor causing soil degradation on sandy soils. The risk of wind erosion will further increase due to climate change. Consequently, understanding the effects of wind erosion on soil and SOC losses is necessary for supporting sustainable soil management and mitigating soil degradation. Our wind tunnel experiments successfully provided first results to quantify and qualify these processes.

Funding source

This study was supported by the German Federal Ministry of Education and Research (BMBF) by funding the research project: Innovative Solutions for Sustainable Agricultural and Climate Adaptation in the Dry Steppes of Kazakhstan and Southwestern Siberia (ReKKS) – grant number 01LZ1704B.

Acknowledgements

We are particularly grateful to Lasse Pein for his contribution to the mobile wind tunnel. Thanks to Timur Kabrulov for his local expertise and support during field experiments. We express our thanks to Dorothee Kley for logistical assistance and Michael von Hoff for conducting laser diffraction analyses. We thank editor Laura Alakukku and the reviewers for their valuable feedback on this manuscript.

Declaration of competing interest

The authors declare that they have no known competing financial interests or personal relationships that could have appeared to influence the work reported in this paper.

Data availability

All data supporting the findings of this study were reviewed and are openly available at https://doi.org/10.4228/ZALF-QQ16-T967.

Appendix

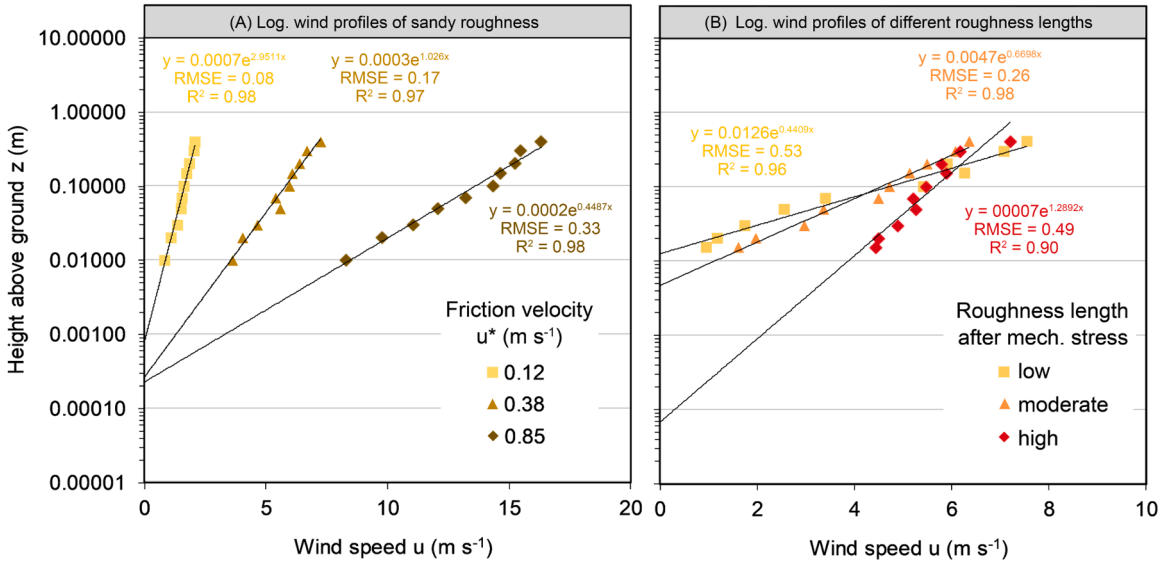

Fig. A1. Logarithmic wind profiles of sandy roughness under three different friction velocities derived from three different wind speeds (A) and logarithmic wind profiles of different roughness lengths (equal wind speed) after low (light cultivator), moderate (disc harrow), and high (tractor tires) mechanical stress application (B).

Table A1
Particle size classes and selected subclasses from topsoil, aeolian sediments, and depositions. The subclasses of fine/coarse clay and very coarse sand are not shown.

Plot	Source	Particle size classes (USDA)			Selected particle size subclasses (USDA)					
		Clay 0 2 µm (%)	Silt 2–50 µm (%)	Sand 50–2000 µm (%)	Fine silt 2–20 µm (%)	Coarse silt 20–50 µm (%)	Very fine sand 50–100 µm (%)	Fine sand 100–200 µm (%)	Medium sand 200–500 µm (%)	Coarse sand 500–1000 µm (%)
1	Topsoil	6	18	76	14	4	12	28	26	9
	Sediment	6	21	73	15	5	16	34	22	1
2	Topsoil	6	18	76	14	4	12	26	28	10
	Sediment	3	11	86	8	3	11	35	36	3
	Deposition	4	10	85	9	2	10	45	30	0
3	Topsoil	4	13	83	10	3	11	29	30	12
	Sediment	3	9	88	7	2	9	33	37	8
	Deposition	4	9	87	8	1	7	37	43	1

Table A2
Aggregate size and modes of motion classes in aeolian sediments collected during wind tunnel experiments.

Plot	MWAC height	Aggregate size classes		Modes of motion classes				
		Micro-aggregates < 250 µm (%)	Macro-aggregates > 250 µm (%)	Long-term suspension < 20 µm (%)	Short-term suspension 20–70 µm (%)	Modified saltation 70–100 µm (%)	Saltation 70–500 µm (%)	Creep > 500 µm (%)
1	Ground level	86	14	2	19	17	78	2
	0.05 m	85	15	4	20	15	74	3
	0.10–0.30 m	83	17	3	29	16	64	4
2	Ground level	80	20	1	13	15	81	5
	0.05 m	83	17	1	12	14	86	2
	0.10–0.35 m	65	35	0	6	8	88	5
3	Ground level	83	17	1	12	15	86	2
	0.05 m	83	17	1	13	15	82	4
	0-10-0.35 m	73	27	0	9	12	85	5

Table A3
Soil organic carbon content from topsoil, aeolian sediments, and depositions, as well as soil organic carbon ratio as content from the eroded material to the content from the topsoil.

Plot	Source	Measured	Calculated	MWAC height	Measured	Calculated
		Soil organic carbon content ($g\ kg^{-1}$)	Soil organic carbon ratio (-)		Soil organic carbon content ($g\ kg^{-1}$)	Soil organic carbon ratio (-)
1	Topsoil	17.8	/	Ground level	20.8	1.17
	Sediment	30.0	1.69	0.05 m	22.3	1.25
				0.10-0.30 m	30.0	1.69
2	Topsoil	14.9	/	Ground level	15.7	1.06
	Sediment	13.0	0.87	0.05 m	15.9	1.07
	Deposition	11.7	0.78	0.10-0.35 m	13.0	0.87
3	Topsoil	13.8	/	Ground level	11.3	0.82
	Sediment	8.9	0.65	0.05 m	11.5	0.83
	Deposition	8.8	0.64	0.10-0.35 m	8.9	0.65

References

Aubekerov, B., Gorbunov, A., 1999. Quaternary permafrost and mountain glaciation in Kazakhstan 16. https://onlinelibrary.wiley.com/doi/10.1002/(SICI)1099-1530(199901/03)10:1%3C65::AID-PPP306%3E3.0.CO;2-X.

Bezak, N., Mikoš, M., Borrelli, P., Alewell, C., Alvarez, P., Anache, J.A.A., Baartman, J., Ballabio, C., Biddoccu, M., Cerdà, A., Chalise, D., Chen, S., Chen, W., De Girolamo, A. M., Gessesse, G.D., Deumlich, D., Diodato, N., Efthimiou, N., Erpul, G., Fiener, P., Freppaz, M., Gentile, F., Gericke, A., Haregeweyn, N., Hu, B., Jeanneau, A., Kaffas, K., Kiani-Harchegani, M., Villuendas, I.L., Li, C., Lombardo, L., López-Vicente, M., Lucas-Borja, M.E., Maerker, M., Miao, C., Modugno, S., Möller, M., Naipal, V., Nearing, M., Owusu, S., Panday, D., Patault, E., Patriche, C.V., Poggio, L., Portes, R., Quijano, L., Rahdari, M.R., Renima, M., Ricci, G.F., Rodrigo-Comino, J., Saia, S., Samani, A.N., Schillaci, C., Syrris, V., Kim, H.S., Spinola, D.N., Oliveira, P.T., Teng, H., Thapa, R., Vantas, K., Vieira, D., Yang, J.E., Yin, S., Zema, D.A., Zhao, G., Panagos, P., 2021. Soil erosion modelling: a bibliometric analysis. Environ. Res. 197, 111087 https://doi.org/10.1016/j.envres.2021.111087.

Bischoff, N., Mikutta, R., Shibistova, O., Puzanov, A., Reichert, E., Silanteva, M., Grebennikova, A., Schaarschmidt, F., Heinicke, S., Guggenberger, G., 2016. Land-use change under different climatic conditions: consequences for organic matter and microbial communities in Siberian steppe soils. Agric., Ecosyst. Environ. 235, 253–264. https://doi.org/10.1016/j.agee.2016.10.022.

Borrelli, P., Alewell, C., Alvarez, P., Anache, J.A.A., Baartman, J., Ballabio, C., Bezak, N., Biddoccu, M., Cerdà, A., Chalise, D., Chen, S., Chen, W., De Girolamo, A.M., Gessesse, G.D., Deumlich, D., Diodato, N., Efthimiou, N., Erpul, G., Fiener, P., Freppaz, M., Gentile, F., Gericke, A., Haregeweyn, N., Hu, B., Jeanneau, A., Kaffas, K., Kiani-Harchegani, M., Villuendas, I.L., Li, C., Lombardo, L., López-Vicente, M., Lucas-Borja, M.E., Märker, M., Matthews, F., Miao, C., Mikoš, M., Modugno, S., Möller, M., Naipal, V., Nearing, M., Owusu, S., Panday, D., Patault, E., Patriche, C.V., Poggio, L., Portes, R., Quijano, L., Rahdari, M.R., Renima, M., Ricci, G.F., Rodrigo-Comino, J., Saia, S., Samani, A.N., Schillaci, C., Syrris, V., Kim, H.S., Spinola, D.N., Oliveira, P.T., Teng, H., Thapa, R., Vantas, K., Vieira, D., Yang, J.E., Yin, S., Zema, D.A., Zhao, G., Panagos, P., 2021. Soil erosion modelling: a global review and statistical analysis. Sci. Total Environ. 780, 146494 https://doi.org/10.1016/j.scitotenv.2021.146494.

Bronick, C.J., Lal, R., 2005. Soil structure and management: a review. Geoderma 124, 3–22. https://doi.org/10.1016/j.geoderma.2004.03.005.

Burri, K., Gromke, C., Lehning, M., Graf, F., 2011. Aeolian sediment transport over vegetation canopies: a wind tunnel study with live plants. Aeolian Res. 3, 205–213. https://doi.org/10.1016/j.aeolia.2011.01.003.

Cerdà, A., Flanagan, D.C., le Bissonnais, Y., Boardman, J., 2009. Soil erosion and agriculture. Soil Tillage Res. 106, 107–108. https://doi.org/10.1016/j.still.2009.10.006.

Chappell, A., Webb, N.P., Butler, H.J., Strong, C.L., McTainsh, G.H., Leys, J.F., Viscarra Rossel, R.A., 2013. Soil organic carbon dust emission: an omitted global source of atmospheric CO_2. Glob. Change Biol. 19, 3238–3244. https://doi.org/10.1111/gcb.12305.

Chepil, W.S., 1952. Factors that Influence Clod Structure and Erodibility of Soil by Wind: 1. Soil Texture.

Chepil, W.S., 1953. Field structure of cultivated soils with special reference to erodibility by wind. Soil Sci. Soc. Am. Proc.

Chepil, W.S., 1960. Conversion of Relative Field Erodibility to Annual Soil Loss by Wind. Soil Science Society of America Proceedings 143–145. https://doi.org/doi.org/10.2136/sssaj1960.03615995002400020022x.

Chepil, W.S., 1962. A compact rotary sieve and importance of dry sieving in physical soil analysis. Soil Sci. Soc. Am. J. 26, 4–6. https://acsess.onlinelibrary.wiley.com/doi/10.2136/sssaj1960.03615995002400020022x.

Colazo, J.C., Buschiazzo, D.E., 2010. Soil dry aggregate stability and wind erodible fraction in a semiarid environment of Argentina. Geoderma 159, 228–236. https://doi.org/10.1016/j.geoderma.2010.07.016.

Dong, Z., Sun, H., Zhao, A., 2004. WITSEG sampler: a segmented sand sampler for wind tunnel test. Geomorphology 59, 119–129. https://doi.org/10.1016/j.geomorph.2003.09.010.

DTU, 2021. Global Wind Atlas 3.1. Technical University of Denmark (DTU Wind Energy), Denmark. Available at: https://globalwindatlas.info/.

Duulatov, E., Chen, X., Issanova, G., Orozbaev, R., Mukanov, Y., Amanambu, A.C., 2021. Current and future trends of rainfall erosivity and soil erosion in Central Asia. SpringerBriefs in Environmental Science. Springer International Publishing, Cham. https://doi.org/10.1007/978-3-030-63509-1.

FAO, 2012. AQUASTAT: Kazakhstan. Food and Agriculture Organization of the United Nations (FAO), Rome, Italy.

FAO, 2014. World reference base for soil resources 2014: international soil classification system for naming soils and creating legends for soil maps. Food and Agriculture Organization of the United Nations (FAO), Rome, Italy.

Field, J.P., Breshears, D.D., Whicker, J.J., 2009. Toward a more holistic perspective of soil erosion: Why aeolian research needs to explicitly consider fluvial processes and interactions. Aeolian Res. 1, 9–17. https://doi.org/10.1016/j.aeolia.2009.04.002.

Frühauf, M., Meinel, T., Schmidt, G., 2020. In: Frühauf, M., Guggenberger, G., Meinel, T., Theesfeld, I., Lentz, S. (Eds.), The Virgin Lands Campaign (1954–1963) Until the Breakdown of the Former Soviet Union (FSU): With Special Focus on Western Siberia. KULUNDA: Climate Smart Agriculture, Innovations in Landscape Research. Springer International Publishing, Cham, pp. 101–118. https://doi.org/10.1007/978-3-030-15927-6_8.

Fryrear, D.W., Saleh, A., Bilbro, J.D., Schomberg, H.M., Stout, J.E., Zobeck, T.M., 1998. Revised Wind Erosion Equation (RWEQ), Wind Erosion and Water Conservation Research Unit, Technical Bulletin No. 1. USDA-ARS, Texas, USA.

Funk, R., Reuter, H.I., 2006. Wind erosion. In: Boardman, J., Poesen, J. (Eds.), Soil Erosion in Europe. John Wiley & Sons, Ltd, Chichester, pp. 563–582. https://doi.org/10.1002/0470859202.ch41.

Funk, R., Engel, W., 2015. Investigations with a field wind tunnel to estimate the wind erosion risk of row crops. Soil Tillage Res. 145, 224–232. https://doi.org/10.1016/j.still.2014.09.005.

Funk, R., Skidmore, E., Hagen, L., 2004. Comparison of wind erosion measurements in Germany with simulated soil losses by WEPS. Environ. Model. Softw. 19, 177–183. https://doi.org/10.1016/S1364-8152(03)00120-8.

Funk, R., Hoffmann, C., Reiche, M., 2014. Methods for quantifying wind erosion in steppe regions. In: Mueller, L., Saparov, A., Lischeid, G. (Eds.), Novel Measurement and Assessment Tools for Monitoring and Management of Land and Water Resources in Agricultural Landscapes of Central Asia. Environmental Science and Engineering. Springer International Publishing, Cham, pp. 315–327. https://doi.org/10.1007/978-3-319-01017-5_18.

Funk, R., Völker, L., Deumlich, D., 2023. Landscape structure model based estimation of the wind erosion risk in Brandenburg, Germany. Aeolian Res. 62, 100878 https://doi.org/10.1016/j.aeolia.2023.100878.

Gardner, W.H., 2018. Water Content. In: Klute, A. (Ed.), SSSA Book Series. Soil Science Society of America, American Society of Agronomy, Madison, WI, USA, pp. 493–544. https://doi.org/10.2136/sssabookser5.1.2ed.c21.

Gregorich, E.G., Greer, K.J., Anderson, D.W., Liang, B.C., 1998. Carbon distribution and losses: erosion and deposition effects. Soil Tillage Res. 47, 291–302. https://doi.org/10.1016/S0167-1987(98)00117-2.

Grunwald, L.-C., Belyaev, V.I., Hamann, M., Illiger, P., Stephan, E., Bischoff, N., Rudev, N.V., Kozhanov, N.A., Schmidt, G., Frühauf, M., Meinel, T., 2016. Modern cropping systems and technologies for soil conservation in siberian agriculture. In: Mueller, L., Sheudshen, A.K., Eulenstein, F. (Eds.), Novel Methods for Monitoring and Managing Land and Water Resources in Siberia. Springer Water. Springer International Publishing, Cham, pp. 681–715. https://doi.org/10.1007/978-3-319-24409-9_31.

Hagen, L.J., 2001. Assessment of wind erosion parameters using wind tunnels. In: Stott, D.E., Mohtar, R.H., Steinhardt, G.C. (Eds.), Sustaining the Global Farm, pp. 742–746.

Harris, I.C., Jones, P.D., Osborn, T., 2020. CRU TS4.04: Climatic Research Unit (CRU) Time-Series (TS) version 4.04 of high-resolution gridded data of month-by-month variation in climate (Jan. 1901- Dec. 2019). Sci Data 7.
Hornbeck, R., 2012. The enduring impact of the american dust bowl: short- and long-run adjustments to environmental catastrophe. Am. Econ. Rev. 102, 1477–1507. https://doi.org/10.1257/aer.102.4.1477.
Iturri, L.A., Buschiazzo, D.E., 2023. Interactions between wind erosion and soil organic carbon. in: Agricultural Soil Sustainability and Carbon Management. Elsevier, pp. 163–179. https://doi.org/10.1016/B978-0-323-95911-7.00005-0.
Janssen, W., Tetzlaff, G., 1991. Construction and calibration of a recording sand trap. (in Geman: Entwicklung und Eichung einer registrierenden Suspensionsfalle). Z. Kult. Landentwickl. 32, 167–179.
Kassam, A., Friedrich, T., Derpsch, R., 2019. Global spread of conservation agriculture. Int. J. Environ. Stud. 76, 29–51. https://doi.org/10.1080/00207233.2018.1494927.
Keesstra, S.D., Bouma, J., Wallinga, J., Tittonell, P., Smith, P., Cerdà, A., Montanarella, L., Quinton, J.N., Pachepsky, Y., van der Putten, W.H., Bardgett, R.D., Moolenaar, S., Mol, G., Jansen, B., Fresco, L.O., 2016. The significance of soils and soil science towards realization of the United Nations Sustainable Development Goals. SOIL 2, 111–128. https://doi.org/10.5194/soil-2-111-2016.
Kienzler, K.M., Lamers, J.P.A., McDonald, A., Mirzabaev, A., Ibragimov, N., Egamberdiev, O., Ruzibaev, E., Akramkhanov, A., 2012. Conservation agriculture in Central Asia—what do we know and where do we go from here? Field Crops Res. 132, 95–105. https://doi.org/10.1016/j.fcr.2011.12.008.
Kok, J.F., Parteli, E.J.R., Michaels, T.I., Karam, D.B., 2012. The physics of wind-blown sand and dust. Rep. Prog. Phys. 75, 106901 https://doi.org/10.1088/0034-4885/75/10/106901.
Koza, M., Funk, R., Schmidt, G., 2023. Wind erosion after steppe conversion inKazakhstan: Data from mobile wind tunnel experiments [Dataset]. Leibniz Centre for Agricultural Landscape Research (ZALF). https://doi.org/10.4228/ZALF-QQ16-T967.
Koza, M., Schmidt, G., Bondarovich, A., Akshalov, K., Conrad, C., Pöhlitz, J., 2021. Consequences of chemical pretreatments in particle size analysis for modelling wind erosion. Geoderma 396, 115073. https://doi.org/10.1016/j.geoderma.2021.115073.
Koza, M., Pöhlitz, J., Prays, A., Kaiser, K., Mikutta, R., Conrad, C., Vogel, C., Meinel, T., Akshalov, K., Schmidt, G., 2022. Potential erodibility of semi-arid steppe soils derived from aggregate stability tests. Eur. J. Soil Sci. 73 (5), e13304 https://doi.org/10.1111/ejss.13304.
Kraemer, R., Prishchepov, A.V., Müller, D., Kuemmerle, T., Radeloff, V.C., Dara, A., Terekhov, A., Frühauf, M., 2015. Long-term agricultural land-cover change and potential for cropland expansion in the former Virgin Lands area of Kazakhstan. Environ. Res. Lett. 10, 054012 https://doi.org/10.1088/1748-9326/10/5/054012.
Lackóová, L., Pokrývková, J., Kozlovsky Dufková, J., Policht-Latawiec, A., Michałowska, K., Dąbrowska, J., 2021. Long-term impact of wind erosion on the particle size distribution of soils in the eastern part of the european union. Entropy 23, 935. https://doi.org/10.3390/e23080935.
Lafond, G.P., May, W.E., Stevenson, F.C., Derksen, D.A., 2006. Effects of tillage systems and rotations on crop production for a thin Black Chernozem in the Canadian Prairies. Soil Tillage Res. 89, 232–245. https://doi.org/10.1016/j.still.2005.07.014.
Lal, R., 2001. Soil degradation by erosion. Land Degrad. Dev. 12, 519–539. https://doi.org/10.1002/ldr.472.
Lal, R., Reicosky, D.C., Hanson, J.D., 2007. Evolution of the plow over 10,000 years and the rationale for no-till farming. Soil Tillage Res. 93, 1–12. https://doi.org/10.1016/j.still.2006.11.004.
Larionov, G.A., 1993. Erosion and deflation of soils: General regularities and quantitative assessment (in Russian: Эрозия и дефляция почв: основные законоМерности и количественные оценки). Moscow State University, Moscow.
Larney, F., 2007. Dry-Aggregate Size Distribution. In: Carter, M., Gregorich, E. (Eds.), Soil Sampling and Methods of Analysis, Second Edition. CRC Press, pp. 821–831. https://doi.org/10.1201/9781420005271.ch63.
Lee, J.A., Gill, T.E., 2015. Multiple causes of wind erosion in the Dust Bowl. Aeolian Res. 19, 15–36. https://doi.org/10.1016/j.aeolia.2015.09.002.
Li, J., Chen, H., Zhang, C., 2020a. Impacts of climate change on key soil ecosystem services and interactions in Central Asia. Ecol. Indic. 116, 106490 https://doi.org/10.1016/j.ecolind.2020.106490.
Li, J., Ma, X., Zhang, C., 2020b. Predicting the spatiotemporal variation in soil wind erosion across Central Asia in response to climate change in the 21st century. Sci. Total Environ. 709, 136060 https://doi.org/10.1016/j.scitotenv.2019.136060.
Li, X.-Y., Liu, L.-Y., Wang, J.-H., 2004. Wind tunnel simulation of aeolian sandy soil erodibility under human disturbance. Geomorphology 59, 3–11. https://doi.org/10.1016/j.geomorph.2003.09.001.
López, M.V., Sabre, M., Gracia, R., Arrúe, J.L., Gomes, L., 1998. Tillage effects on soil surface conditions and dust emission by wind erosion in semiarid Aragón (NE Spain). Soil and Tillage Research 45, 91–105. https://doi.org/10.1016/S0167-1987(97)00066-4.
López, M.V., de Dios Herrero, J.M., Hevia, G.G., Gracia, R., Buschiazzo, D.E., 2007. Determination of the wind-erodible fraction of soils using different methodologies. Geoderma 139, 407–411. https://doi.org/10.1016/j.geoderma.2007.03.006.
Marzen, M., Kirchhoff, M., Marzolff, I., Aït Hssaine, A., Ries, J.B., 2020. Relative quantification of wind erosion in argan woodlands in the Souss Basin, Morocco. Earth Surf. Process. Landf. 45, 3808–3823. https://doi.org/10.1002/esp.5002.
Maurer, T., Herrmann, L., Gaiser, T., Mounkaila, M., Stahr, K., 2006. A mobile wind tunnel for wind erosion field measurements. J. Arid Environ. 66, 257–271. https://doi.org/10.1016/j.jaridenv.2005.11.002.
McLeman, R.A., Dupre, J., Berrang Ford, L., Ford, J., Gajewski, K., Marchildon, G., 2014. What we learned from the Dust Bowl: lessons in science, policy, and adaptation. Popul Environ. 35, 417–440. https://doi.org/10.1007/s11111-013-0190-z.
Meier, U., 2018. Growth stages of mono- and dicotyledonous plants: BBCH Monograph. Open Agrar Repositorium, Quedlingburg.https://doi.org/10.5073/20180906–074619.
Meinel, T., Akshalov, K., 2015. Development of land use management in the Eurasian steppe area: from moldboard to direct seeding (in Russian: Степи Северной Еразии: Материалы VII МеЖдународного сиМпозиуМа). In: Chibilev, A.A. (Ed.), Steppes of Northern Eurasia: Materials of VII International Symposium. Publishing House “Dimur”, Orenburg, pp. 64–66.
Meinel, T., Grunwald, L.-C., Akshalov, K., 2014. Modern technologies for soil management and conservation in Northern Kazakhstan. In: Mueller, L., Saparov, A., Lischeid, G. (Eds.), Novel Measurement and Assessment Tools for Monitoring and Management of Land and Water Resources in Agricultural Landscapes of Central Asia, Environmental Science and Engineering. Springer International Publishing, Cham, pp. 455–464. https://doi.org/10.1007/978-3-319-01017-5_27.
Meteoblue, 2023. Simulated historical climate and weather data. Basel. Available at: https://www.meteoblue.com/en/weather/historyclimate/climatemodelled/.
Montgomery, D.R., 2007. Soil erosion and agricultural sustainability. Proc. Natl. Acad. Sci. U. S. A. 104, 13268–13272. https://doi.org/10.1073/pnas.0611508104.
Nerger, R., Funk, R., Cordsen, E., Fohrer, N., 2017. Application of a modeling approach to designate soil and soil organic carbon loss to wind erosion on long-term monitoring sites (BDF) in Northern Germany. Aeolian Res. 25, 135–147. https://doi.org/10.1016/j.aeolia.2017.03.006.
Peters, D.P., Groffman, P.M., Nadelhoffer, K.J., Grimm, N.B., Collins, S.L., Michener, W. K., Huston, M.A., 2008. Living in an increasingly connected world: a framework for continental-scale environmental science. Front. Ecol. Environ. 6, 229–237. https://doi.org/10.1890/070098.
Podsiadłowski, S.T., 1988. Wind erosion of light soil in the wheel tracks of a farm tractor. J. Agric. Eng. Res. 39, 231–243. https://doi.org/10.1016/0021-8634(88)90145-X.
Prishchepov, A.V., Schierhorn, F., Dronin, N., Ponkina, E.V., Müller, D., 2020. 800 Years of Agricultural Land-use Change in Asian (Eastern) Russia. In: Frühauf, M., Guggenberger, G., Meinel, T., Theesfeld, I., Lentz, S. (Eds.), KULUNDA: Climate Smart Agriculture, Innovations in Landscape Research. Springer International Publishing, Cham, pp. 67–87. https://doi.org/10.1007/978-3-030-15927-6_6.
Pye, K., 1994. Sediment transport and depositional processes. Blackwell Scientific Publications, Oxford; Boston.
R. Core Team, 2020. A language and environment for statistical computing. R Foundation for Statistical Computing, Vienna. Available at: https://www.r-project.org/.
Reyer, C.P.O., Otto, I.M., Adams, S., Albrecht, T., Baarsch, F., Cartsburg, M., Coumou, D., Eden, A., Ludi, E., Marcus, R., Mengel, M., Mosello, B., Robinson, A., Schleussner, C.-F., Serdeczny, O., Stagl, J., 2017. Climate change impacts in Central Asia and their implications for development. Reg. Environ. Change 17, 1639–1650. https://doi.org/10.1007/s10113-015-0893-z.
Reynolds, J.F., Smith, D.M.S., Lambin, E.F., Turner, B.L., Mortimore, M., Batterbury, S.P. J., Downing, T.E., Dowlatabadi, H., Fernández, R.J., Herrick, J.E., Huber-Sannwald, E., Jiang, H., Leemans, R., Lynam, T., Maestre, F.T., Ayarza, M., Walker, B., 2007. Global desertification: building a science for dryland development. Science 316, 847–851. https://doi.org/10.1126/science.1131634.
Robinson, S., 2016. Land degradation in central asia: evidence, perception and policy. In: Behnke, R., Mortimore, M. (Eds.), Springer Earth System Sciences, The End of Desertification?. Springer Berlin Heidelberg, Berlin, Heidelberg, pp. 451–490. https://doi.org/10.1007/978-3-642-16014-1_17.
Scheffer, F., Schachtschabel, P., Blume, H.-P., 2016. Soil science, first ed. Springer, Berlin.
Shahabinejad, N., Mahmoodabadi, M., Jalalian, A., Chavoshi, E., 2019. In situ field measurement of wind erosion and threshold velocity in relation to soil properties in arid and semiarid environments. Environ. Earth Sci. 78, 501 https://doi.org/10.1007/s12665-019-8508-5.
Shao, Y. (Ed.), 2008. Physics and modelling of wind erosion, Atmospheric and oceanographic sciences library. Springer, Cambridge.
Shao, Y., Wyrwoll, K.-H., Chappell, A., Huang, J., Lin, Z., McTainsh, G.H., Mikami, M., Tanaka, T.Y., Wang, X., Yoon, S., 2011. Dust cycle: an emerging core theme in Earth system science. Aeolian Res. 2, 181–204. https://doi.org/10.1016/j.aeolia.2011.02.001.
Sirjani, E., Sameni, A., Moosavi, A.A., Mahmoodabadi, M., Laurent, B., 2019. Portable wind tunnel experiments to study soil erosion by wind and its link to soil properties in the Fars province, Iran. Geoderma 333, 69–80. https://doi.org/10.1016/j.geoderma.2018.07.012.
Soil Science Division Staff, 2017. Soil survey manual, eighteenth ed. Government Printing Office, Washington, D.C, USA.
Stolbovoi, V., 2000. Soils of Russia: Correlated with the Revised Legend of the FAO Soil Map of the World and World Reference Base for Soil Resources. International Institute for Applied Systems Analysis, Laxenburg, Austria.
Suleimenov, M., Kaskarbayev, Z., Akshalov, K., Tulegenov, A., 2016. Principles of conservation agriculture in continental steppe regions. In: Mueller, L., Sheudshen, A. K., Eulenstein, F. (Eds.), Novel Methods for Monitoring and Managing Land and Water Resources in Siberia. Springer Water. Springer International Publishing, Cham, pp. 667–679. https://doi.org/10.1007/978-3-319-24409-9_30.
Taiyun, W., Simko, V., 2021. R package “corrplot”: Visualization of a correlation matrix (version 0.92).
Tanner, S., Katra, I., Haim, A., Zaady, E., 2016. Short-term soil loss by eolian erosion in response to different rain-fed agricultural practices. Soil Tillage Res. 155, 149–156. https://doi.org/10.1016/j.still.2015.08.008.

Tisdall, J.M., Oades, J.M., 1982. Organic matter and water-stable aggregates in soils. Eur. J. Soil Sci. 33, 141–163. https://doi.org/10.1111/j.1365-2389.1982.tb01755.x.
Van Pelt, R.S., Zobeck, T.M., 2013. Portable wind tunnels for field testing of soils and natural surfaces. In: Ahmed, N. (Ed.), Wind tunnel designs and their diverse engineering applications. InTech. https://doi.org/10.5772/54141.
Verhulst, N., Govaerts, B., Verachtert, E., Castellanos-Navarrete, A., Mezzalama, M., Wall, P.C., Chocobar, A., Deckers, J., Sayre, K.D., 2010. Conservation agriculture, improving soil quality for sustainable production systems? In: Lal, R., Stewart, B.A. (Eds.), Food Security and Soil Quality. CRC Press, pp. 137–208. https://doi.org/10.1201/EBK1439800577-7.
Webb, N.P., Kachergis, E., Miller, S.W., McCord, S.E., Bestelmeyer, B.T., Brown, J.R., Chappell, A., Edwards, B.L., Herrick, J.E., Karl, J.W., Leys, J.F., Metz, L.J., Smarik, S., Tatarko, J., Van Zee, J.W., Zwicke, G., 2020. Indicators and benchmarks for wind erosion monitoring, assessment and management. Ecol. Indic. 110, 105881 https://doi.org/10.1016/j.ecolind.2019.105881.
White, B.R., Mounla, H., 1991. An experimental study of Froude number effect on wind-tunnel saltation. In: Barndorff-Nielsen, O.E., Willetts, B.B. (Eds.), Aeolian Grain Transport 1, Acta Mechanica Supplementum. Springer, Vienna, pp. 145–157. https://doi.org/10.1007/978-3-7091-6706-9_9.
Wieringa, J., 1992. Updating the Davenport roughness classification. J. Wind Eng. Ind. Aerodyn. 41, 357–368. https://doi.org/10.1016/0167-6105(92)90434-C.
Yan, Y., Wang, X., Guo, Z., Chen, J., Xin, X., Xu, D., Yan, R., Chen, B., Xu, L., 2018. Influence of wind erosion on dry aggregate size distribution and nutrients in three steppe soils in northern China. CATENA 170, 159–168. https://doi.org/10.1016/j.catena.2018.06.013.
Yin, C., Zhao, W., Pereira, P., 2022. Soil conservation service underpins sustainable development goals. Glob. Ecol. Conserv. 33, e01974 https://doi.org/10.1016/j.gecco.2021.e01974.
Yost, J.L., Hartemink, A.E., 2019. Soil organic carbon in sandy soils: a review. in: Advances in Agronomy. Elsevier, pp. 217–310. https://doi.org/10.1016/bs.agron.2019.07.004.
Zamani, S., Mahmoodabadi, M., 2013. Effect of particle-size distribution on wind erosion rate and soil erodibility. Arch. Agron. Soil Sci. 59, 1743–1753. https://doi.org/10.1080/03650340.2012.748984.
Zenchelsky, S.T., Delany, A.C., Pickett, R.A.I., 1976. The organic component of wind-blown soil aerosol as a function of wind velocity. Soil Sci. 122, 129–132.
Zepner, L., Karrasch, P., Wiemann, F., Bernard, L., 2021. ClimateCharts.net – an interactive climate analysis web platform. Int. J. Digit. Earth 14, 338–356. https://doi.org/10.1080/17538947.2020.1829112.
Zhang, C.-L., Zou, X.-Y., Gong, J.-R., Liu, L.-Y., Liu, Y.-Z., 2004. Aerodynamic roughness of cultivated soil and its influences on soil erosion by wind in a wind tunnel. Soil Tillage Res. 75, 53–59. https://doi.org/10.1016/S0167-1987(03)00159-4.
Zobeck, T.M., Fryrear, D.W., 1986. Chemical and physical characteristics of windblown sediment II. chemical characteristics and total soil and nutrient discharge. Trans. ASAE 29, 1037–1041. https://doi.org/10.13031/2013.30266.
Zobeck, T.M., Popham, T.W., 1990. Dry aggregate size distribution of sandy soils as influenced by tillage and precipitation. Soil Sci. Soc. Am. J. 54, 198–204. https://doi.org/10.2136/sssaj1990.03615995005400010031x.
Zobeck, T.M., Van Pelt, R.S., 2015. Wind erosion. In: Hatfield, J.L., Sauer, T.J. (Eds.), Soil Management: Building a Stable Base for Agriculture. Soil Science Society of America, Madison, WI, USA, pp. 209–227. https://doi.org/10.2136/2011.soilmanagement.c14.
Zobeck, T.M., Baddock, M., Scott Van Pelt, R., Tatarko, J., Acosta-Martinez, V., 2013. Soil property effects on wind erosion of organic soils. Aeolian Res. 10, 43–51. https://doi.org/10.1016/j.aeolia.2012.10.005.
Zobeck, T.M., Sterk, G., Funk, R., Rajot, J.L., Stout, J.E., Van Pelt, R.S., 2003. Measurement and data analysis methods for field-scale wind erosion studies and model validation. Earth Surf. Process. Landf. 28, 1163–1188. https://doi.org/10.1002/esp.1033.